Responses to Referee Comments #1 and #2

We would like to thank both referees for their very helpful comments regarding our manuscript. Below we have included our responses. The referee comments are in black text while our responses are in blue.

Referee Comment #1

This paper estimates the effective absorbing optical property of “brown carbon” (BrC), which is a part of the bulk primary organic carbon (POC) emitted from biomass burning, by adjusting the spectral dependence of imaginary refractive indices of BrC and BrC/POC ratio in the GEOS-Chem simulation of UVAI to match the UVAI from OMI and reported AAE from literature. Then, the consequences of BrC absorption on tropospheric OH and aerosol direct radiative effects (DRE) are calculated with the GEOS-Chem model, which show significant reduction of OH and changes of DRE over major biomass burning regions/seasons.

1. The term “primarily non-absorbing” or “primarily scattering” for OC is somewhat misleading. The imaginary refractive indices (k) of OC from OPAC is 0.005 – 0.008 in the 300-550 nm wavelength range, which means OC is absorbing, at least weakly absorbing. In fact, the k value of OC increases with the wavelength from 350 to NIR (about 0.4 at ⇠9000 nm), therefore OC should not be defined as non-absorbing aerosol even with the OPAC values. The problem seems mostly in the UV and shortwave VIS range where the absorption from OPAC is likely to be too weak and the AAE too low.

We now avoid the terms “primarily non-absorbing” or “primarily scattering”.

2. The relationship between k and BrC/POC ratio shown in Table 2 and Figure 3 is quite confusing. For example, at 350 nm, k=0.005 at BrC/POC=0, and it increases to 0.077 (0.11) at BrC/POC=0.5, but then it decreases to 0.037 (0.051) when the BrC/POC ratio further increases to 1. That sounds counterintuitive - should k increase with the fraction of BrC? Why should it go the opposite direction?

Thank you for identifying this source of confusion. For the base case, k was for all POC. For case 2, k was for BrC alone (not all POC). To eliminate this confusion, we have separated Table 2 into two tables, have modified the caption of Figure 3, and have modified the text.

Table 2: Imaginary part of the refractive index (*k*) values for the base case with weakly absorbing “colorless” primary organic carbon.

Wavelength (nm)	**Base Case**
300	0.008
350	0.005
400	0.005
450	0.005
500	0.005
550	0.006

Table 5: Imaginary part of the refractive index (*k*) values for brown carbon (not total organic carbon) inferred for case 2. We include *k* values associated with multiple densities (ρ), and multiple fractions of

brown carbon to primary organic carbon (BrC/POC). All four columns for case 2 yield the same absorption.

	Case 2 with BrC (ρ = 1.3 g cm^{-3})		**Case 2 with BrC (ρ = 1.8 g cm^{-3})**	
Wavelength (nm)	**BrC/POC = 0.50**	**BrC/POC = 1.0**	**BrC/POC = 0.50**	**BrC/POC=1.0**
300	0.11	0.051	0.16	0.071
350	0.077	0.037	0.11	0.051
400	0.052	0.025	0.073	0.035
450	0.035	0.014	0.049	0.019
500	0.023	0.009	0.032	0.013
550	0.015	0.007	0.021	0.010

I understand that you use the UVAI as a constraint; you have to choose a combination of k and BrC/POC ratio, i.e., if you use a higher k then you would have to use a lower BrC/POC ratio and vice versa, in order to match the same UVAI with OMI. However, this also means that you cannot independently obtain the k or BrC/POC ratio (and BrC density as well) from UVAI, since the four columns of case 2 in Table 2 give you exactly the same UVAI. What is the catch here? This question really should be explicitly discussed in the manuscript.

The catch is that this method eliminates the need to know the BrC/POC ratio. The effective value of k can be inferred for the assumed BrC/POC ratio. We added on line 610 of the revised manuscript, “This effective refractive index of BrC eliminates the need to know the BrC/POC ratio to model the radiative effects of BrC.”

To obtain the k values for BrC through our sensitivity simulations, we assume a fixed spectral dependence and BrC/POC fraction, then we adjust the magnitude of the k values in order to reproduce the absorption observed by OMI for the different BrC/POC cases.

In order to clarify our approach, following lines 431-433:

“Through sensitivity simulations, we derive the effective *k* values for BrC and the BrC/POC fraction required to reproduce the observed absorption by the OMI UVAI.”

We add:

“This is accomplished by conducting the sensitivity simulations for several cases of BrC/POC fraction and assuming the same fixed spectral dependence for each case. We then adjust the magnitude of the effective *k* values to match the OMI UVAI.”

At line 448 we also add the sentence: “The effective *k* values increase with decreasing BrC/POC fraction because as BrC concentration decreases, BrC must be more absorbing to match the absorption observed by OMI.”

These changes should make our method clearer to the reader.

3. Related to the question above, what BrC/POC ratio is used in computing UVAI in Figure 4? If it does not matter as far as you use the consistent pair of k and BrC/POC (and density) to reproduce the UVAI, what is your recommendation to other models to use, especially not every model will be able to compute the UVAI in order to select the pair of k and BrC/POC?

The reviewer is correct that the choice of BrC/POC ratio is irrelevant as long as a consistent pair of k and

BrC/POC ratio is chosen. The relationship between k and BrC/POC ratio was derived so that others will be able to choose which fraction makes the most sense to them scientifically, and will then be able to calculate the k value associated with that fraction. We leave the choice of BrC/POC ratio to the user's discretion. We added to line 612, "Rather, an effective refractive index can be chosen (eq. 6) to represent an internal mixture of BrC and colorless POC."

We also add to line 471, "The columns with effective *k* values for BrC/POC fraction of unity offer the convenience of representing the effective absorption by BrC without needing to assume an arbitrary BrC/POC fraction, or to introduce a separate BrC tracer. The effective *k* values for unity BrC/POC fraction can be thought of as the effective imaginary refractive index for an internal mixture of BrC and colorless POC."

Other comments:

Page 27411, line 23, "where k is the intercept": Intercept of what? I think you meant that log(k) is the intercept of linear fitting of log(AAOD) and log(lambda).

The exponential relationship relating AAOD and AAE is: $\text{AAOD} = k\lambda^{-\text{AAE}}$, where k is just an arbitrary constant that is not important for the calculation of AAE from the AAOD vs λ relationship in log-log space.

Page 27411, line 23 (line 281 in the revised manuscript,) we have changed "where k is the intercept."

To:

"where k is a constant."

Referee Comment #2

This paper uses satellite measurements and model simulations to constrain the optical properties of absorbing organic aerosol (brown carbon), and estimate changes to photo-oxidation and the aerosol direct radiative effect. The authors first show that in a model simulation with only weakly/non-absorbing organic carbon, the ultraviolet aerosol index is biased low relative to satellite measurements. Next, the authors use satellite observations to estimate the wavelength-dependent imaginary index of refraction for brown carbon. This is then used in GEOS-Chem to estimate changes to OH production and the direct radiative effect. The paper is suitable for publication with some minor comments.

It is stated that Figures 1-3 are monthly mean UVAI. I am unclear, though, if you supplied monthly-mean aerosol fields to VLIDORT and calculated the UVAI or calculated UVAI at a higher temporal resolution (daily?) and then took the average. If the former do you expect much difference (perhaps from cloud or snow cover)?

On page 12 line 328 we now state that we use daily aerosol fields at satellite overpass time.

Section 4.2 contains a good deal of information; however, I found it a little hard to follow. The first two paragraphs of Section 4.2 contain background information and could possibly be moved to the introduction. It's not clear how the effective imaginary index of refraction is determined. I think a few more sentences elaborating on the methods of estimating the imaginary index of refraction for brown carbon are needed (this could perhaps be moved to the 'methods' - Section 3, and the results remain in Section 4?). The background and methods described here (in my opinion) tend to disrupt the flow of the results.

Helpful suggestion. We have moved paragraphs from the start of sec. 4.2 to the introduction.

It is difficult to tell the difference between the color of the filled circles and background colors in Figure 3 (I realize this is partly the point). A thicker edge color may help.

We have added a thicker edge color to the circles in Figure 3.

I believe GC-RT assumes externally mixed aerosols. As you are considering an absorbing (and hydrophilic) species, an internal mixture may lead to slightly more absorption. I doubt this would change your general point, but it may be useful to state.

On page 12 line 341 we have added: "Aerosols are treated as externally mixed."

Tables 1 and 5 are a little difficult to compare. Is there a way to combine them? The paragraph in the text is clearly written (and could possibly stand on its own). You could consider moving the tables and Section 2.2 to the supplement, but that's just a suggestion.

Table 1 has the headings of each wavelength region we considered in our Absorbing Angstrom Exponent (AAE) analysis, then lists below the literature references falling within that wavelength range. We provide the mean and standard deviation of the literature references for each wavelength region, to compare with our AAE analysis in Table 5 (Table 6 in the revised manuscript). We do not wish to include a supplement with this paper.

In addition to addressing the reviewer comments, we also correct a minor error in the calculation of the change in OH and DRE.

Interpreting the Ultraviolet Aerosol Index Observed with the OMI Satellite Instrument to Understand Absorption by Organic Aerosols: Implications for Atmospheric Oxidation and Direct Radiative Effects

Melanie S. Hammer[1], Randall V. Martin[1,2], Aaron van Donkelaar[1], Virginie Buchard[3,4], Omar Torres[3], David A. Ridley[5], Robert J.D. Spurr[6]

[1]Department of Physics and Atmospheric Science, Dalhousie University, Canada

[2]Harvard-Smithsonian Center for Astrophysics, Cambridge, MA, USA

[3]NASA/Goddard Space Flight Center, Greenbelt, MD, USA

[4]GESTAR/Universities Space Research Association, Columbia, MD, USA

[5]Department of Civil and Environmental Engineering, Massachusetts Institute of Technology, Cambridge, MA, USA

[6]RT Solutions, Inc., 9 Channing Street, Cambridge, MA 02138, USA

Correspondence to: M. S. Hammer (melanie.hammer@dal.ca)

Abstract

Satellite observations of the Ultraviolet Aerosol Index (UVAI) are sensitive to absorption of solar radiation by aerosols; this absorption affects photolysis frequencies and radiative forcing. We develop a global simulation of the UVAI using the 3-D chemical transport model GEOS-Chem coupled with the Vector Linearized Discrete Ordinate Radiative Transfer model (VLIDORT). The simulation is applied to interpret UVAI observations from the Ozone Monitoring Instrument (OMI) for the year 2007. Simulated and observed values are highly consistent in regions where mineral dust dominates the UVAI, but a large negative bias (-0.32 to -0.97) exists between simulated and observed values in biomass burning regions. We determine effective optical properties for absorbing organic aerosol, known as brown carbon (BrC), and implement them into GEOS-Chem to better represent observed UVAI values over biomass burning regions. The inclusion~~addition~~ of absorbing BrC decreases the mean bias between simulated and OMI UVAI values from -0.57 to -0.09 over West Africa in January, from -0.32 to +0.0002 over South Asia in April, from -0.97 to -0.22 over southern Africa in July, and from -0.50 to +0.33 over South

America in September. The spectral dependence of absorption after including~~adding~~ BrC in~~to~~ the model is broadly consistent with reported observations for biomass burning aerosol, with Absorbing Angstrom Exponent (AAE) values ranging from 2.9 in the ultraviolet (UV) to 1.3 across the UV-Near IR spectrum. We assess the effect of the additional UV absorption by BrC on atmospheric photochemistry by examining tropospheric hydroxyl radical (OH) concentrations in GEOS-Chem. The inclusion of BrC decreases OH by up to 25% over South America in September, up to 20% over southern Africa in July, and up to 13% over other biomass burning regions. Global annual mean OH concentrations in GEOS-Chem decrease due to the presence of absorbing BrC, increasing the methyl chloroform lifetime from 5.62 years to 5.66 years, thus reducing the bias against observed values. We calculate the direct radiative effect (DRE) of BrC using GEOS-Chem coupled with the radiative transfer model RRTMG (GC-RT). Treating organic aerosol as containing more strongly absorbing BrC~~ rather than as primarily scattering ~~changes the global annual mean all-sky top of atmosphere (TOA) DRE by +0.02 W m^{-2} and all-sky surface DRE by -0.06 W m^{-2}. Regional changes of up to +0.25 W m^{-2} at TOA and down to -1 W m^{-2} at the surface are found over major biomass burning regions.

1 Introduction

Absorption of solar radiation by aerosols plays a major role in radiative forcing and atmospheric photochemistry. Aerosol absorption has been estimated to be the second largest source of radiative forcing after carbon dioxide (Bond et al., 2013; IPCC, 2014; Ramanathan and Carmichael, 2008), although considerable uncertainty remains regarding the magnitude of the forcing (Stier et al., 2007; Wang et al., 2014). Absorption of ultraviolet (UV) radiation by aerosols decreases photolysis frequencies, leading to a reduction in the concentrations of atmospheric oxidants (Dickerson et al., 1997; Jacobson, 1998; Liao et al., 2003; Martin et al., 2003). Many atmospheric chemistry models tend to overestimate tropospheric hydroxyl radical (OH) concentrations compared to observations (Mao et al., 2013; Naik et al., 2013). Accurately representing aerosol absorption could help rectify the discrepancies between simulated and observed OH concentrations, and offer constraints on radiative forcing.

The Ultraviolet Aerosol Index (UVAI) is a method of detecting aerosol absorption using satellite measurements. The UVAI is calculated by separating the spectral contrast of radiances due to aerosol effects from those due to Rayleigh scattering at two wavelengths in the near-UV region (Herman et al., 1997; Torres et al., 1998, 2007). Two attributes of the UVAI method are 1) that aerosol optical properties are more readily detected over surfaces with low reflectance such as found in the UV (Torres et al., 2005), and 2) that the strong interaction between aerosol absorption and molecular scattering in the near-UV increases the sensitivity of UV-radiances to aerosol absorption (Torres et al., 1998). These attributes enhance the ability of the UVAI to detect aerosol absorption that affects UV photolysis and radiative forcing.

Traditionally, black carbon (BC) is treated as the ~~sole~~ predominant absorbing carbonaceous aerosol, and all organic carbon is assumed to be primarily scattering or weakly absorbing colorless aerosol. However, a growing number of observations have found evidence of significant absorption by a subset of organic carbon, known as "brown carbon" (BrC), which is strongest in the ultraviolet and decreases into the visible and near-IR wavelength regions (Bergstrom et al., 2007; Chen and Bond, 2010; Kirchstetter et al., 2004; Martins et al., 2009; Yang et al., 2008; Zhong and Jang, 2014). The majority of BrC is emitted to the atmosphere through low-temperature, incomplete combustion of biomass and biofuel (Chen and Bond, 2010; Kirchstetter et al., 2004; Zhong and Jang, 2014). There is evidence of a possible source from residential coal burning (Bond, 2001), while the high-temperature environment associated with other fossil fuel combustion is unfavorable to BrC formation (Andreae and Gelencsér, 2006; Saleh et al., 2014). BrC has been observed to contribute significantly to the overall absorption by biomass burning aerosol, especially in the UV (Clarke et al., 2007; Corr et al., 2012; Kirchstetter and Thatcher, 2012). The UVAI is sensitive to this absorption (Jethva and Torres, 2011).

A great deal of uncertainty exists regarding the fraction of total primary organic carbon that is brown (BrC/POC). This uncertainty arises from the variety of methods used to measure BrC absorption as well as the variable nature of organic aerosols themselves (Lack and Langridge, 2013). Filter-based measurements where the organic carbon is extracted from the total biomass burning aerosol sample with the use of solvents range from 50-90% (Chen and Bond, 2010; Kirchstetter et al., 2004). A broad range of BrC/POC values have been used to simulate absorption by brown carbon. For example, Feng et al. (2013) assume 66% of primary organic carbon from biomass and biofuel emissions is brown, Wang et al. (2014) assume 50% of POC from biomass and 25% of POC from biofuel emissions is brown, while Lin et al. (2014) assume 100% POC from biomass and biofuel emissions is brown. Global observations of reflected solar radiation used in the UVAI could offer a constraint on these different assumptions.

Several estimates of BrC absorption exist, but they all differ significantly. The imaginary part of the refractive index (*k*) for BrC derived by Kirchstetter et al. (2004) and Chen and Bond (2010) are often taken, respectively, as the upper ($k \sim 0.168$ at 350 nm) and lower ($k \sim 0.074$ at 350 nm) limits in modelling studies (Arola et al., 2011; Feng et al., 2013; Lin et al., 2014). Different observations may reflect different burn conditions (Saleh et al., 2014) as well as chemical loss and evaporation of BrC (Forrister et al., 2015; Zhong and Jang, 2014). Global observations are needed to infer the effective absorption across a variety of conditions.

Many~~Several~~ studies have estimated the direct radiative effect (DRE) and/or direct radiative forcing (DRF) by BrC. In Heald et al. (2014) a clear distinction is made between the DRE, which is the instantaneous imbalance of out-going longwave and incoming shortwave radiation due to the presence of an atmospheric constituent, and the DRF, which is the difference in DRE between present-day and preindustrial conditions. Prior estimates of the change in all-sky top of atmosphere (TOA) DRE from treating organic aerosol as containing BrC ~~brown rather than primarily scattering~~ range from +0.04 W m^{-2} to +0.25 W m^{-2} globally (Chung et al., 2012; Feng et al., 2013), with estimates of regional seasonal DRE of organic aerosol including absorbing BrC ranging from +0.5-1 W m^{-2} (Arola et al., 2015). Most studies estimate a TOA DRF between 0.07 and 0.57 W m^{-2} due to absorption by BrC (Lin et al., 2014; Park et al., 2010; Wang et al., 2014). Following submission of our manuscript, we learned of a submitted manuscript by Jo et al., (2015) that developed a global simulation of BrC and applied it to investigate atmospheric photochemistry. To our knowledge, this work and that by Jo et al., (2015) ~~no~~are the first two chemical transport modeling studies that have considered the effect of absorption by BrC on atmospheric photochemistry.

In this work we introduce brown carbon to the chemical transport model GEOS-Chem and examine its effect on atmospheric absorption and photochemistry, in particular in known biomass burning regions. To evaluate aerosol absorption, section 3 develops a simulation of the UVAI following Buchard et al. (2015) using the Vector Linearized Discrete Radiative Transfer model (VLIDORT) coupled with aerosol fields from GEOS-Chem. Section 4 compares the simulated UVAI values to observations from the Ozone Monitoring Instrument (OMI). The change in reflected solar radiation as observed by the UVAI tests the effective representation of the absorption of UV radiation by BrC. Section 5 examines the effect of the added BrC absorption on ozone photolysis frequencies and tropospheric OH concentrations in the GEOS-Chem simulation. Section 6 calculates the DRE of absorbing brown carbon. Section 7 reports the conclusions.

2 Observations

2.1 OMI Ultraviolet Aerosol Index

The OMI Ultraviolet Aerosol Index is a method of detecting absorbing aerosols from satellite measurements in the near-UV wavelength region. The UVAI was first observed from the Nimbus-7 TOMS (Total Ozone Mapping Spectrometer) (Herman et al., 1997; Torres et al., 1998) and is currently a product of the OMI Near-UV algorithm (OMAERUV) (Torres et al., 2007). OMI flies on NASA's Aura satellite and has been taking global daily measurements since 2004. The OMAERUV algorithm uses the 354 and 388 nm radiances measured by OMI to calculate the UVAI according to Torres et al. (1998, 2007):

$$\mathrm{UVAI} = -\,100\log_{10}\left[\frac{I_{354}^{\mathrm{meas}}}{I_{354}^{\mathrm{calc}}\left(R_{354}^{*}\right)}\right] \tag{1}$$

where I_{354}^{meas} is the TOA at 354 nm as measured by OMI, and I_{354}^{calc} is the radiance at 354 nm calculated for a purely Rayleigh scattering atmosphere bounded by a Lambertian surface of reflectance R_{354}^{*}, which is known as the adjusted Lambert Equivalent Reflectivity (LER) (Dave, 1978). R_{354}^{*} is calculated by correcting the LER at 388 nm (R_{388}^{*}) for the spectral dependence of the surface reflectance at 354 nm.

Positive UVAI values indicate absorbing aerosol. Negative values indicate non-absorbing aerosol. Near-zero values indicate clouds, minimal aerosol, or other non-aerosol related effects such as unaccounted for land surface albedo wavelength dependence, ocean color effects or specular ocean reflection (i.e. sun glint). These second order effects yield UVAI values ± 0.5 within the noise level (Torres et al., 2007). The OMAERUV product identifies clouds using the measured scene reflectivity and the UVAI (Torres et al., 2013). We reject cloudy conditions (quality flag of 1) to focus on cloud free conditions (quality flag 0).

In this work we use the OMI UVAI to evaluate simulated UVAI values, as described in section 3.

2.2 Absorption Angstrom Exponent (AAE)

We use observations of the Absorption Angstrom Exponent (AAE) for biomass burning aerosol to test our representation of the spectral dependence of absorption. The AAE is the slope of aerosol absorption optical depth (AAOD) versus wavelength (λ) in log-log space. Using the AAE, the AAOD can be related to wavelength with the power-law relationship

$$\mathrm{AAOD} = k\lambda^{-\mathrm{AAE}} \qquad (2),$$

where k is a constant. Aerosols with spectrally independent absorption display an AAE of about 1, while aerosols with spectrally dependent absorption have an AAE > 1. BC exhibits spectrally independent absorption, and is often accepted as having an AAE close to 1 (Bergstrom et al., 2002; Bond and Bergstrom, 2006). The observed AAE over the near-UV to near-IR spectral regions can indicate aerosol type, with urban pollution aerosols dominated by BC exhibiting an AAE near 1, biomass burning aerosols displaying an AAE near 2, and desert dust having an AAE > 2 (Bergstrom et al., 2007; Russell et al., 2009).

Several recent studies have attributed the spectrally dependent absorption by biomass burning aerosols to the presence of BrC (Clarke et al., 2007; Corr et al., 2012; Kirchstetter and Thatcher, 2012; Rizzo et al., 2011; Zhong and Jang, 2014). Kirchstetter et al. (2004) measured over the 300-1000 nm range an AAE of ~ 2 for biomass burning aerosol and an AAE of ~ 1 for motor vehicle aerosol. They found that after extracting the organic carbon from the samples using acetone, the AAE of the biomass burning aerosol decreased to around 1, while the motor vehicle aerosol AAE remained unchanged. They concluded that the spectral dependence of absorption by biomass burning aerosol was due to BrC, while the absorption by motor vehicle emissions was due to BC.

Table 1 contains a summary of measured AAE values for biomass burning aerosol. AAE values increase toward UV wavelengths as expected for BrC absorption. Variability in the AAE at visible wavelengths may reflect differences in burn conditions and fuel type. Observations in the ultraviolet, such as the UVAI, offer an exciting opportunity to exploit the large AAE of biomass burning aerosol at short wavelengths to assess the global magnitude of BrC absorption (Jethva and Torres, 2011).

3. Simulated Ultraviolet Aerosol Index

We simulate the UVAI following Buchard et al. (2015) using the VLIDORT model (Spurr, 2006), which includes polarization effects and uses the discrete ordinates method to solve the radiative transfer equation. We supply VLIDORT with the OMI pixel viewing geometry to calculate the UVAI for that pixel. The UVAI values are calculated from TOA radiances computed by VLIDORT at 354 and 388 nm, the wavelengths used by the OMAERUV product.

Following Buchard et al. (2015) we calculate simulated UVAI values as:

$$\mathrm{UVAI} = -\,100\log_{10}\left[\frac{I_{354}^{\mathrm{RAY+AER}}}{I_{354}^{\mathrm{RAY}}\left(R_{354}^{*}\right)}\right] \tag{3}$$

where $I_{354}^{\mathrm{RAY+AER}}$ is the TOA radiance calculated with VLIDORT at 354 nm assuming an atmosphere containing aerosol and Rayleigh effects, and I_{354}^{RAY} is the TOA radiance calculated with VLIDORT at 354 nm assuming a purely Rayleigh scattering atmosphere bounded by a Lambertian surface of reflectance R_{354}^{*} (adjusted Lambert Equivalent Reflectivity).

R_{354}^{*} is calculated by correcting the Lambert Equivalent Reflectivity at 388 nm (R_{388}^{*}) for wavelength dependence:

$$R_{354}^{*} = R_{388}^{*} - (R_{388} - R_{354}) \tag{4}$$

where R_{388} and R_{354} are surface reflectance values from a revisited TOMS-based climatology dataset (Torres et al., 2013).

R_{388}^{*} is calculated by relating TOA radiance to diffuse reflectivity using the equation (Buchard et al., 2015):

$$R_{388}^{*} = \frac{I_{388}^{\mathrm{RAY+AER}} - I_{388}^{\mathrm{RAY}}}{T_{388}^{\mathrm{RAY}} + S_{b_{388}}^{\mathrm{RAY}}\left(I_{388}^{\mathrm{RAY+AER}} - I_{388}^{\mathrm{RAY}}\right)} \tag{5}$$

where $I_{388}^{\mathrm{RAY+AER}}$ is the TOA radiance calculated with VLIDORT at 388 nm assuming an atmosphere containing aerosol and Rayleigh effects, I_{388}^{RAY} is the TOA radiance at 388 nm calculated with VLIDORT for a purely Rayleigh scattering atmosphere bounded by a Lambertian surface, T_{388}^{RAY} is the simulated transmittance at 388 nm for a Rayleigh atmosphere, and $S_{b_{388}}^{\mathrm{RAY}}$ is the spherical albedo of a Rayleigh atmosphere at 388 nm.

For the calculation of TOA radiances, we provide VLIDORT with vertical profiles of aerosol extinction, single scattering albedo, and 32 Legendre-function expansion coefficients of the scattering phase function. We assume all aerosol particles are spherical. We obtain these aerosol optical properties using daily aerosol fields at satellite overpass time from GEOS-Chem version 9-01-03 (http://geos-chem.org), a global three dimensional chemical transport model driven by assimilated meteorological data from the Goddard Earth Observation System (GEOS-5) of the NASA Global Modeling and Assimilation Office (GMAO). Our simulation is conducted at a spatial resolution of 2°x2.5° with 47 vertical levels for the year 2007.

GEOS-Chem contains a detailed oxidant-aerosol chemical mechanism (Bey et al., 2001; Park et al., 2004). The aerosol simulation includes the sulfate-nitrate-ammonium system (Fountoukis and Nenes, 2007; Park et al., 2004; Pye et al., 2009), primary carbonaceous aerosol (Park et al., 2003), ~~secondary organic aerosol (Henze and Seinfeld, 2006; Henze et al., 2008; Liao et al., 2007),~~ mineral dust (Fairlie et al., 2007), and sea salt (Jaeglé et al., 2011). Aerosol optical properties are based on the Global Aerosol Data Set (GADS) (Köepke et al., 1997) as implemented by Martin et al., (2003), with updates for organics and secondary inorganics from aircraft observations (Drury et al., 2010), and for mineral dust (Lee et al., 2009; Ridley et al., 2012). Aerosols are treated as externally mixed. We treat the density of organic aerosol as 1.3 g cm^{-3} (Duplissy et al., 2011; Kuwata et al., 2012) and assume an organic aerosol mass to organic carbon fraction of 2.1 (Aiken et al., 2008; Canagaratna et al., 2015; Turpin and Lim, 2001).

Anthropogenic emissions are from the EDGAR v32-FT2000 global inventory for 2000 (Olivier et al., 2005) with emissions overwritten in areas with regional inventories for the United States (NEI 2005), Mexico (BRAVO; Kuhns et al., 2005), Europe (EMEP; http://www.emep.int/), and East Asia (Zhang et al., 2009). Emissions are scaled to the year 2007 following emissions of related CO_2 sources as described in van Donkelaar et al. (2008). Global biofuel emissions (Yevich and Logan, 2003), global anthropogenic emissions for carbonaceous aerosols (Bond et al., 2007; Leibensperger et al., 2012), and emissions from open fires for individual years from the GFED3 inventory (Mu et al., 2011) are included.

We calculate UVAI values for two cases. The base case simulation treats the aerosol optical properties as currently implemented in GEOS-Chem in which all organic carbon aerosols are ~~primarily scattering~~ weakly absorbing and colorless as shown in Table 2. The second case adds the more strongly absorbing BrC as described in section 4.2 below.

4 Comparison of simulated and OMI UVAI

4.1 Base case simulation

Figure 1 shows the monthly mean OMI UVAI observations for January, April, July, and September of 2007. Clear signals are apparent over regions dominated by mineral dust and biomass burning (Herman et al., 1997; Torres et al., 1998). Absorption over desert regions occurs for all four months, giving UVAI values between 1 and 3, particularly over the Saharan, Iranian, and Thar deserts. Aerosol absorption from biomass burning primarily follows the seasonal cycle of agricultural burning (Duncan et al., 2003). In January, absorption over West Africa yields UVAI values between 1 and 2.5. In April aerosol absorption is visible over South Asia with UVAI values between 0.5 and 1. UVAI values of 1-1.7 occur over southern Africa in both July and September, while UVAI values of up to 3 occur over South America in September.

Figure 2 shows the monthly mean UVAI values for our base case simulation without BrC.~~which treats organic carbon aerosol as primarily non-absorbing~~. The simulation captures the major absorption features compared to OMI over the desert regions, giving UVAI values of 1-3, however it fails to capture the absorption by biomass burning aerosol, giving UVAI values between -2 and 0 in all biomass burning regions for the four months. These negative values indicate that the UVAI simulation is insensitive to the absorption by BC and is dominated by the scattering from organic carbon aerosol. A sensitivity test with doubled BC concentrations increased UVAI values by only ~0.1. We also conducted a sensitivity test to determine if the heights of the biomass burning plumes could explain the underestimated absorption. Raising the aerosol layer height to unrealistic altitudes (~10 km above the surface) increased the UVAI by only 0.1-0.3, which is insufficient to account for the differences between the simulation and observations.

To further analyze the discrepancies between simulated and observed UVAI, we choose four regions corresponding to the seasonal biomass burning outlined in Figure 1: West Africa (5°S-25°N, 40°W-20°E) in January, South Asia (5-35°N, 60-110°E) in April, southern Africa (0-30°S, 5°W-30°E) in July, and South America (0-40°S, 40-70°W) in September. Table 3 contains the correlation coefficients (r) between the simulated and OMI UVAI as well as the mean bias (simulated-OMI UVAI). The correlation between the OMI and simulated UVAI is low (0.09-0.48) in all regions, with large mean biases of -0.32 to -0.97

Uncertainty in aerosol optical depth also cannot explain the UVAI bias. Table 4 shows the simulated AOD compared with AOD retrieved from the MODIS (Moderate Resolution Imaging Spectroradiometer) and MISR (Multi-angle Imaging Spectroradiometer) satellite instruments. Overall the simulated values are within the range of satellite retrieved AOD values. The maximum difference in simulated versus satellite AOD is found with the MODIS Dark Target algorithm over South America in September. Matching the simulated AOD to the satellite AOD changed the UVAI by less than 0.1.

We attempt to reconcile the differences between the simulated and OMI UVAI in biomass burning regions by introducing absorbing BrC into GEOS-Chem, as described below.

4.2 Treatment of brown carbon

~~A great deal of uncertainty exists regarding the fraction of total primary organic carbon that is brown (BrC/POC). This uncertainty arises from the variety of methods used to measure BrC absorption as well as the variable nature of organic aerosols themselves. BrC absorption is often measured by subtracting the absorption attributed to black carbon from the total measured aerosol absorption, and attributing the difference to BrC (e.g. Arola et al., 2011; Yang et al., 2009). Lack and Langridge (2013) argue that this method is subject to the uncertainties associated with the measured absorption of BC as well as the possible presence of absorbing mineral dust. Filter-based measurements where the organic carbon is extracted from the total biomass burning aerosol sample with the use of solvents provide a more robust estimate (Liu et al., 2013). Chen and Bond (2010) used methanol to extract organic carbon from a variety of burning wood samples generated in a laboratory and found that 92% of the total organic carbon present in the samples was brown. Kirchstetter et al. (2004) extracted organic carbon from biomass burning samples taken in southern Africa using acetone and found that 50-80% of the total organic carbon could be attributed to BrC. A broad range of BrC/POC values have been used to simulate absorption by brown carbon. For example, Feng et al. (2013) assume 66% of primary organic carbon from biomass and biofuel emissions is brown, Wang et al. (2014) assume 50% of POC from biomass and 25% of POC from~~

~~biofuel emissions is brown, while Lin et al. (2014) assume 100% POC from biomass and biofuel emissions is brown.~~

~~Evidence for the existence of brown secondary organic carbon (Br-SOA) also exists. The majority of Br-SOA is from anthropogenic sources (Liu et al., 2013, 2014; Zhang et al., 2013), while SOA formed from biogenic carbon is largely non-absorbing (Flores et al., 2014; Liu et al., 2014). On a global scale it is estimated that the majority of SOA is formed from biogenic carbon (Hallquist et al., 2009; Lack et al., 2004; Tsigaridis and Kanakidou, 2003). Therefore we treat SOA as non-absorbing. We tested this approach in a sensitivity study by assigning 100% SOA as brown, and found that the contribution to overall absorption by SOA was negligible (UVAI changed by less than 0.1).~~

~~Several estimates of BrC absorption exist, but they all differ significantly. The imaginary part of the refractive index (k) for BrC derived by Kirchstetter et al. (2004) and Chen and Bond (2010) are often taken, respectively, as the upper (k ~ 0.168 at 350 nm) and lower (k ~ 0.074 at 350 nm) limits in modelling studies (Arola et al., 2011; Feng et al., 2013; Lin et al., 2014). Different observations may reflect different burn conditions (Saleh et al., 2014) as well as chemical loss and evaporation of BrC (Forrister et al., 2015; Zhong and Jang, 2014).~~

Here we apply the OMI UVAI observations to estimate the effective absorption by BrC. We exploit the fact that the TOA radiances used in the OMI UVAI ~~retrievals~~ contain implicit information on the BrC from actual burn conditions, on the BrC that remains after chemical loss or evaporation, on Br-SOA, and on the BrC/POC fraction. We use the term effective to denote the implicit dependence of the UVAI upon these multiple processes. Through sensitivity simulations, we derive the effective k values for BrC ~~and~~given the assumed BrC/POC fraction required to reproduce the observed absorption by the OMI UVAI. This is accomplished by conducting the sensitivity simulations for several cases of BrC/POC fraction, assuming the same fixed spectral dependence for each case, and adjusting the magnitude of the effective k values to match the OMI UVAI. We treat the relative spectral dependence of k, $\log(\Delta k)/\log(\Delta\lambda)$, as 3 for wavelengths between 300 and 600 nm to represent the mean from laboratory and field measurements of 3.2 ± 0.7 (Kirchstetter et al., 2004; Zhang et al., 2013; Zhong and Jang, 2014). At wavelengths ≥ 600 nm we leave the absorption properties of POC unchanged since BrC absorption decreases significantly into the visible and near-IR (Bergstrom et al., 2007; Chen and Bond, 2010; Yang et al., 2008).

The filled circles in Figure 3 show the effective *k* values of BrC derived from seven sensitivity simulations that all achieve the same simulated UVAI. Only the BrC/POC fraction varies between simulations. The choice of simulated UVAI was selected to represent the global OMI UVAI over major biomass burning regions. The imaginary part of the refractive index decreases with increasing wavelength following an exponential relationship as prescribed based on laboratory and field measurements, and decreases with increasing BrC/POC fraction as required to reproduce the OMI UVAI. The effective *k* values increase with decreasing BrC/POC fraction because as BrC concentration decreases, BrC must be more absorbing to match the absorption observed by OMI. Given the smoothly varying relationship between *k* and BrC/POC we develop the following expression to represent this relationship:

$$k = c \cdot \rho \cdot \lambda \cdot \left[35.4 \left(\frac{BrC}{POC}\right)^{-1.25} \cdot \exp(-10.5\lambda)\right]\text{; BrC/POC} \geq 0.4,\ 300\text{ nm} \leq \lambda \leq 600\text{ nm} \qquad (6),$$

where λ is wavelength (μm), ρ is the density of organic carbon (g μm^{-3}), and c is a conversion constant equal to 1.0x10^{12}/4π μm^2 g^{-1}.

The background spectrum of Figure 3 shows the *k* values calculated using Eq. (6). This expression reproduces the full radiative transfer sensitivity simulations with a root mean squared error (RMSE) of 0.004 and a coefficient of determination (r^2) ~~value~~ of 0.99. Equation (6) does not apply for BrC/POC fractions less than 0.4 since they do not reproduce the absorption observed by OMI. We emphasize that multiple choices of *k* and BrC/POC will yield the same TOA radiance and UVAI. The effects on tropospheric OH concentrations and radiative forcing remain unaffected as BrC/POC and effective *k* vary together, since the distribution of scattering and absorption remains the same.

Table 5 contains our derived imaginary parts of the refractive index for BrC/POC fractions of 0.5 and 1.0.~~, compared to the *k* values for non-absorbing organic carbon used in our base case simulation~~. Table 5 also contains effective k values derived for an organic carbon density of 1.8 g cm^{-3} which has been assumed in prior studies of BrC. The range of values for k covered by varying the BrC/POC fraction encompasses the range of values for BrC found in the literature (Chen and Bond, 2010; Feng et al., 2013; Kirchstetter et al., 2004; Lin et al., 2014; Sun et al., 2007; Wang et al., 2014; Zhang et al., 2013; Zhong and Jang, 2014). The four columns with BrC yield identical wavelength dependent global distributions of scattering and absorption that in turn yield the same UVAI, OH, and DRE.

The columns with effective *k* values for BrC/POC fraction of unity offer the convenience of representing the effective absorption by BrC without needing to assume an arbitrary BrC/POC fraction, or to introduce a separate BrC tracer. The effective *k* values for unity BrC/POC fraction can be thought of as the effective imaginary refractive index for an internal mixture of BrC and colorless POC.

Evidence for the existence of brown secondary organic carbon (Br-SOA) also exists. The majority of Br-SOA is from anthropogenic sources (Jo et al., 2015; Liu et al., 2013, 2014; Zhang et al., 2013), while SOA formed from biogenic carbon is largely non-absorbing (Flores et al., 2014; Liu et al., 2014). On a global scale it is estimated that the majority of SOA is formed from biogenic carbon (Hallquist et al., 2009; Lack et al., 2004; Tsigaridis and Kanakidou, 2003). Therefore we treat SOA as non-absorbing. We tested this approach in a sensitivity study with the standard SOA mechanism in GEOS-Chem v9-01-03 (Henze and Seinfeld, 2006; Henze et al., 2008; Liao et al., 2007) by assigning 100% anthropogenic SOA as brown, and found that the change in UVAI was negligible (less than 0.1). Alternative SOA implementations (e.g. as used in Jo et al., 2015) may have a larger effect.

4.3 Simulation including brown carbon

Figure 4 shows the monthly mean UVAI values for the simulation including brown carbon for the months of January, April, July, and September of 2007. The simulated absorption features including BrC are much more consistent than the base case simulation at reproducing the OMI UVAI over biomass burning regions (Figure 2). The simulated UVAI in the four biomass burning regions now ranges from 0.5-3. As summarized in Table 3~~3~~, the correlation coefficients between the simulated and OMI UVAI for the four biomass burning regions now range from 0.57-0.68, with mean biases of -0.22 to +0.33.

The simulated UVAI using global mean *k* values underestimates the OMI observations for the West Africa and southern Africa regions, but overestimates observations in the South American region. We tested how *k* would need to change to explain the regional UVAI bias if *k* were the only error source. We find that these regional biases could be eliminated by changing *k* at 350 nm by +2% over West Africa, by +10% over southern Africa, and by -30% over South America. The presence of more absorbing BrC over West and southern Africa where savannah fires dominate, and less absorbing BrC over the South America region where forest fires dominate, is consistent with work by Saleh et al. (2014) that found the absorptivity of BrC from biomass burning is greater for flaming fires associated with burning grasslands than for smouldering fires associated with burning forest.

The absorption in the West and southern Africa cases appears to be concentrated closer to the source for the simulated values (Figure 4) compared to the OMI values (Figure 1), which show an even distribution of UVAI values away from the source. By contrast, the absorption in the South American region appears to be distributed farther from the source in the simulation than in the OMI observations. Evidence exists of atmospheric photochemical loss and evaporation of brown carbon that causes it to become less absorbing over a lifetime of less than a day (Forrister et al., 2015; Zhong and Jang, 2014). Representing these processes would improve the simulation in the South American region but degrade the simulation in the West Africa and southern Africa regions. Regional treatment of BrC loss processes may be warranted in future work. The current implementation offers our best representation of the effective BrC absorption at the global scale.

Table 6 shows the calculated AAE values for biomass burning aerosol (i.e. black carbon + organic carbon aerosol) from our simulations for comparison with the literature values in Table 1. Large biases are apparent for the base case simulation without BrC. We evaluate the case 2 simulation including BrC in detail. For the 350-400 nm wavelength region our mean AAE value of 2.8±0.22 for the four biomass burning regions is within the recommended values of 2.5-3.0 by Jethva and Torres (2011). In the 350-700 nm range our mean AAE of 2.2±0.17 is close to the value of 1.9 from Kirchstetter and Thatcher (2012). The slight positive bias could arise from the fact that Kirchstetter and Thatcher (2012) took their absorption measurements from wood smoke emitted from houses in rural California during the winter, which have different conditions than the tropical open burning considered here. We obtain a mean AAE value of 1.7 ± 0.15 for the 300-1000 nm range, which falls within the literature values of 1.1 to 2. For the 450-550 nm wavelength region, we obtain a mean AAE value of 2.5 ± 0.14, which is biased high compared to the values from Corr et al. (2012) extracted from an examination of biomass burning plumes in North-Central

Canada, where burn conditions differ from the mostly tropical regions considered in our analysis. Over the 400-700 nm region we obtain a mean AAE of 2.1 ± 0.15, falling within the range of the literature values (1.3-2.1). In the 400-1000 nm region, we obtain a mean AAE value of 1.3 ± 0.005, which is at the low end of the literature values (1.3-1.7). The overall consistency between observed and simulated AAE provides a measure of confidence in spectral dependence of aerosol optical properties from the UV to the IR. We now examine the implications of this absorption for OH and DRE.

5. Analysis of the effect of absorption by BrC on OH concentrations in GEOS-Chem

The strong absorption in the UV by brown carbon aerosol decreases photolysis frequencies, which has implications for ozone photolysis and OH production. Here we examine the effect of the added absorption by BrC on the $O^3 \rightarrow O(^1D)$ photolysis frequency, $J(O(^1D))$, and tropospheric OH concentrations.

Figure 5 shows the percent differences in lower tropospheric OH concentrations between the GEOS-Chem simulation including absorbing brown carbon versus the base case simulation. ~~with primarily scattering organic carbon.~~ The most significant decreases correspond with the major biomass burning regions. The addition of BrC decreases OH concentrations by up to 25% over the South American biomass burning region in September and up to 20% over the southern Africa biomass burning region in July. OH concentrations decrease by up to 13% over West Africa in January and southern Africa in September, with decreases of up to 5% over North America in July, South America in July, and South Asia in January, April, and September~~all four months~~. The spatial and seasonal pattern of $J(O^1(D))$ differences closely reproduces the changes in OH (r^2 = 0.85) (not shown).

Methyl chloroform observations provide a valuable constraint on global OH (Prather et al., 2012; Spivakovsky et al., 2000). The addition of BrC to the GEOS-Chem simulation reduces global mean tropospheric OH concentrations. The reduction in global mean OH concentrations increases the methyl chloroform lifetime to tropospheric OH from 5.62 years to 5.66 years. This change is noteworthy given the buffered nature of OH. This change slightly reduces the bias with observations giving a methyl chloroform lifetime of 6.0 (+0.5, -0.4) years (Prinn et al., 2005).

6. Radiative impact of brown carbon

We calculate the direct radiative effect (DRE) of including absorbing BrC relative to that of the ~~non-absorbing organic carbon assumed in our~~ base case simulation. We use GEOS-Chem coupled with the radiative transfer model RRTMG (Iacono et al., 2008), a configuration known as GC-RT, that is described in Heald et al. (2014). GC-RT calculates both the longwave (LW) and shortwave (SW) instantaneous total radiative fluxes as well as the flux differences due to a specific constituent of the atmosphere (e.g. organic aerosol). The DRE is calculated by adding the LW and SW flux differences determined through perturbation of the constituent of interest. Our GC-RT simulations use version 10.1 of GEOS-Chem with the same aerosol emissions described in section 3 (e.g. GFED3 open fire emissions). We calculate the DRE of absorption by BrC as the difference in the DRE of organic aerosol when including BrC (Case 2) minus the DRE of organic aerosol in the ~~when assuming non-absorbing organic carbon (~~base case~~)~~. We focus on the DRE rather than the DRF to avoid ambiguity in preindustrial BrC.

Figure 6 shows all-sky DRE values for 2007. The top two panels are the DRE values for organic aerosol from the case 2 simulation including BrC. The overall DRE of organic aerosol including BrC is negative, with the largest effects over major biomass burning regions. The bottom two panels show the DRE for absorption by BrC, calculated as the difference between the DRE of organic aerosol for the case 2 simulation including BrC minus the base case simulation.~~ with non-absorbing organic carbon.~~ At the surface BrC absorption reduces the DRE by -1.25 Wm^{-2} over South America and southern Africa, and by -0.5 to -0.25 Wm^{-2} over South Asia, North America, West Africa, Australia, and Europe. At TOA, BrC absorption increases~~reduces~~ the DRE by up to 0.28 Wm^{-2} over South America and southern Africa, and by 0.05 to 0.15 Wm^{-2} over broad regions. This overall cooling effect at the surface and ~~a~~ warming effect on the atmosphere ~~is~~ are consistent with previous work (e.g. Chen and Bond, 2010).

Table 7 contains LW and SW global annual mean flux differences as well as the resulting DRE values for both organic aerosol and brown carbon absorption. The values for organic aerosol are from the base case simulation assuming ~~non-absorbing~~ weakly absorbing organic carbon and the case 2 simulation including BrC, while the values for BrC absorption are calculated as their difference. Absorption by BrC has a mean all-sky DRE at TOA of +0.02 W m^{-2} and at the surface of -0.06 W m^{-2}.

Our findings are at the lower end of the range of values from other studies that estimate the DRE of BrC absorption. Feng et al. (2013) introduce absorption by BrC based on the optical properties from Kirchstetter et al. (2004) and Chen and Bond (2010) into a global model, and calculate an all-sky TOA DRE for BrC absorption of 0.04 to 0.11 W m^{-2}, and an all-sky surface DRE for BrC absorption of -0.06 to -0.14 W m^{-2}. Chung et al. (2012) estimate BrC absorption by subtracting the absorption by BC and desert dust from total aerosol AAE values from AERONET to calculate an all-sky TOA DRE for organic aerosol when including BrC between -0.15 and +0.12 W m^{-2} and an all-sky surface DRE between -1.50 and -0.75 W m^{-2}. Arola et al. (2015) use AERONET retrieved imaginary parts of the refractive index for brown carbon at 440, 670, 870, and 1020 nm to estimate over the Indo-Gangetic plain monthly all-sky TOA DRE values for organic aerosol including BrC absorption up to +0.5 W m^{-2} in spring and as low as -1 W m^{-2} in the winter.

7. Conclusion

We interpret OMI observations of the Ultraviolet Aerosol Index (UVAI), which provides a measure of absorbing aerosols, by developing a simulation of the UVAI using the vector radiative transfer model VLIDORT coupled with GEOS-Chem aerosol fields. The base case simulation without brown carbon (BrC)~~, which treats organic carbon as primarily scattering,~~ well represents the observed UVAI in most of the world but significantly underestimates the absorption in biomass burning regions. We apply the OMI UVAI to estimate absorption by ~~brown carbon (~~BrC~~)~~. This approach exploits the strong absorption by BrC at ultraviolet wavelengths and its effect on top of atmosphere (TOA) radiance. We express the imaginary part of the refractive index of BrC that is required to obtain near-identical TOA radiance values as a function of the fraction of primary organic carbon that is brown. This effective refractive index of BrC ~~and effective BrC fraction~~ provides a measure of the degree of browness needed to represent the complex processes (e.g. burn conditions, photochemical loss) affecting global BrC and in turn the UVAI. This effective refractive index of BrC eliminates the need to know the BrC/POC ratio to model the radiative effects of BrC. Rather, an effective refractive index can be chosen (eq. 6) to represent an internal mixture of BrC and colorless POC.

The simulation including absorbing BrC is much more consistent than the base case at reproducing the OMI UVAI over biomass burning regions. The mean bias between simulated and

OMI UVAI values is reduced from -0.57 to -0.09 over West Africa in January, from -0.32 to +0.0002 over South Asia in April, from -0.97 to -0.22 over southern Africa in July, and from -0.50 to +0.33 over South America in September. The updated optical properties for BrC result in AAE values for biomass burning aerosol ranging from 2.9 in the UV to 1.3 across the UV-Near IR, which are broadly consistent with field observations.

We apply this constraint on ultraviolet absorption to examine implications for the $O_3 \rightarrow O(^1D)$ photolysis frequency. We find that the inclusion of absorbing BrC into GEOS-Chem decreases $J(O(^1D))$ and lower tropospheric OH by up to 25% over South America in September, up to 20% over southern Africa in July, up to 13% over West Africa in January and southern Africa in September, and up to 5% elsewhere. The decrease in global mean OH concentration in GEOS-Chem increases the methyl chloroform lifetime to tropospheric OH from 5.62 years to 5.66 years, slightly reducing the bias with estimates from observations of 6.0 (+0.5, -0.4) years.

We calculate the direct radiative effect (DRE) of BrC using GEOS-Chem coupled with the radiative transfer model RRTMG (GC-RT). We obtain global annual mean all-sky TOA DRE values for BrC absorption of 0.02 Wm^{-2} and values of -0.06 Wm^{-2} at the surface. Regional changes of up to +0.25 W m^{-2} at TOA and down to -1 W m^{-2} at the surface are found over major biomass burning regions. Our results are within the range of prior estimates of DRE for BrC absorption.

Ample opportunities exist to further develop the simulations of BrC and more generally of the UVAI. These opportunities include explicitly accounting for the range of processes affecting BrC such as burn conditions, photochemical loss, secondary production, as well as regional treatment of BrC. An explicit simulation of BrC (e.g. Jo et al. (2015)) would facilitate these developments. Interpretation of the long observational record of the UVAI from 1979 to the present should offer constraints on trends in aerosol composition, ultraviolet absorption, and radiative effects. The forthcoming TROPOMI instrument and geostationary constellation (e.g. TEMPO, Sentinel-4, and GEMS) will offer UVAI observations at 5-20 times higher spatial resolution, as well as information on diurnal variation, both of which may offer additional constraints on BrC evolution.

Acknowledgements: This work was supported by the Natural Science and Engineering Research Council of Canada. Computational facilities were provided in part by the Atlantic Computational

Excellence Network consortium of Compute Canada. We thank Farhan Khan for assistance during the early stages of this work.

References

Aiken, A. C., DeCarlo, P. F., Kroll, J. H., Worsnop, D. R., Huffman, J. A., Docherty, K. S., Ulbrich, I. M., Mohr, C., Kimmel, J. R., Sueper, D., Sun, Y., Zhang, Q., Trimborn, A., Northway, M., Ziemann, P. J., Canagaratna, M. R., Onasch, T. B., Alfarra, M. R., Prevot, A. S. H., Dommen, J., Duplissy, J., Metzger, A., Baltensperger, U. and Jimenez, J. L.: O/C and OM/OC Ratios of Primary, Secondary, and Ambient Organic Aerosols with High-Resolution Time-of-Flight Aerosol Mass Spectrometry, Environ. Sci. Technol., 42(12), 4478–4485, doi:10.1021/es703009q, 2008.

Andreae, M. O. and Gelencsér, A.: Black carbon or brown carbon? The nature of light-absorbing carbonaceous aerosols, Atmos. Chem. Phys., 6(10), 3131–3148, doi:10.5194/acp-6-3131-2006, 2006.

Arola, A., Schuster, G., Myhre, G., Kazadzis, S., Dey, S. and Tripathi, S. N.: Inferring absorbing organic carbon content from AERONET data, Atmos. Chem. Phys., 11(1), 215–225, doi:10.5194/acp-11-215-2011, 2011.

Arola, A., Schuster, G. L., Pitkänen, M. R. A., Dubovik, O., Kokkola, H., Lindfors, A. V., Mielonen, T., Raatikainen, T., Romakkaniemi, S., Tripathi, S. N. and Lihavainen, H.: Measurement-based direct radiative effect by brown carbon over Indo-Gangetic Plain, Atmos. Chem. Phys. Discuss., 15(15), 21583–21606, doi:10.5194/acpd-15-21583-2015, 2015.

Bergstrom, R. W., Russell, P. B. and Hignett, P.: Wavelength Dependence of the Absorption of Black Carbon Particles: Predictions and Results from the TARFOX Experiment and Implications for the Aerosol Single Scattering Albedo, J. Atmos. Sci., 59(3), 567–577, doi:10.1175/1520-0469(2002)059<0567:WDOTAO>2.0.CO;2, 2002.

Bergstrom, R. W., Pilewskie, P., Russell, P. B., Redemann, J., Bond, T. C., Quinn, P. K. and Sierau, B.: Spectral absorption properties of atmospheric aerosols, Atmos. Chem. Phys., 7(23), 5937–5943, doi:10.5194/acp-7-5937-2007, 2007.

Bey, I., Jacob, D. J., Yantosca, R. M., Logan, J. A., Field, B. D., Fiore, A. M., Li, Q., Liu, H. Y., Mickley, L. J. and Schultz, M. G.: Global modeling of tropospheric chemistry with assimilated meteorology: Model description and evaluation, J. Geophys. Res., 106(D19), 23073, doi:10.1029/2001JD000807, 2001.

Bond, T. C.: Spectral dependence of visible light absorption by carbonaceous particles emitted from coal combustion, Geophys. Res. Lett., 28(21), 4075–4078, doi:10.1029/2001GL013652, 2001.

Bond, T. C. and Bergstrom, R. W.: Light Absorption by Carbonaceous Particles: An Investigative Review, Aerosol Sci. Technol., 40(1), 27–67, doi:10.1080/02786820500421521, 2006.

Bond, T. C., Bhardwaj, E., Dong, R., Jogani, R., Jung, S., Roden, C., Streets, D. G. and Trautmann, N. M.: Historical emissions of black and organic carbon aerosol from energy-related combustion, 1850-2000, Global Biogeochem. Cycles, 21(2), GB2018, doi:10.1029/2006GB002840, 2007.

Bond, T. C., Doherty, S. J., Fahey, D. W., Forster, P. M., Berntsen, T., DeAngelo, B. J., Flanner,

M. G., Ghan, S., Kärcher, B., Koch, D., Kinne, S., Kondo, Y., Quinn, P. K., Sarofim, M. C., Schultz, M. G., Schulz, M., Venkataraman, C., Zhang, H., Zhang, S., Bellouin, N., Guttikunda, S. K., Hopke, P. K., Jacobson, M. Z., Kaiser, J. W., Klimont, Z., Lohmann, U., Schwarz, J. P., Shindell, D., Storelvmo, T., Warren, S. G. and Zender, C. S.: Bounding the role of black carbon in the climate system: A scientific assessment, J. Geophys. Res. Atmos., 118(11), 5380–5552, doi:10.1002/jgrd.50171, 2013.

Buchard, V., da Silva, A. M., Colarco, P. R., Darmenov, A., Randles, C. A., Govindaraju, R., Torres, O., Campbell, J. and Spurr, R.: Using the OMI aerosol index and absorption aerosol optical depth to evaluate the NASA MERRA Aerosol Reanalysis, Atmos. Chem. Phys., 15(10), 5743–5760, doi:10.5194/acp-15-5743-2015, 2015.

Canagaratna, M. R., Jimenez, J. L., Kroll, J. H., Chen, Q., Kessler, S. H., Massoli, P., Hildebrandt Ruiz, L., Fortner, E., Williams, L. R., Wilson, K. R., Surratt, J. D., Donahue, N. M., Jayne, J. T. and Worsnop, D. R.: Elemental ratio measurements of organic compounds using aerosol mass spectrometry: characterization, improved calibration, and implications, Atmos. Chem. Phys., 15(1), 253–272, doi:10.5194/acp-15-253-2015, 2015.

Chen, Y. and Bond, T. C.: Light absorption by organic carbon from wood combustion, Atmos. Chem. Phys., 10(4), 1773–1787, doi:10.5194/acp-10-1773-2010, 2010.

Chung, C. E., Ramanathan, V. and Decremer, D.: Observationally constrained estimates of carbonaceous aerosol radiative forcing., Proc. Natl. Acad. Sci. U. S. A., 109(29), 11624–9, doi:10.1073/pnas.1203707109, 2012.

Clarke, A., McNaughton, C., Kapustin, V., Shinozuka, Y., Howell, S., Dibb, J., Zhou, J., Anderson, B. E., Brekhovskikh, V., Turner, H. and Pinkerton, M.: Biomass burning and pollution aerosol over North America: Organic components and their influence on spectral optical properties and humidification response, J. Geophys. Res. Atmos., 112(12), 1–13, doi:10.1029/2006JD007777, 2007.

Corr, C. A., Hall, S. R., Ullmann, K., Anderson, B. E., Beyersdorf, A. J., Thornhill, K. L., Cubison, M. J., Jimenez, J. L., Wisthaler, A. and Dibb, J. E.: Spectral absorption of biomass burning aerosol determined from retrieved single scattering albedo during ARCTAS, Atmos. Chem. Phys., 12(21), 10505–10518, doi:10.5194/acp-12-10505-2012, 2012.

Dave, J. V: Effect of Aerosols on the Estimation of Total Ozone in an Atmospheric Column from the Measurements of Its Ultraviolet Radiance, J. Atmos. Sci., 35(5), 899–911, doi:10.1175/1520-0469(1978)035<0899:EOAOTE>2.0.CO;2, 1978.

Dickerson, R. R., Kondragunta, S., Stenchikov, G., Civerolo, K. L., Doddridge, B. G. and Holben, B. N.: The impact of aerosols on solar ultraviolet radiation and photochemical smog., Science, 278(5339), 827–830, doi:10.1126/science.278.5339.827, 1997.

van Donkelaar, A., Martin, R. V., Leaitch, W. R., Macdonald, A. M., Walker, T. W., Streets, D. G., Zhang, Q., Dunlea, E. J., Jimenez, J. L., Dibb, J. E., Huey, L. G., Weber, R. and Andreae, M. O.: Analysis of aircraft and satellite measurements from the Intercontinental Chemical Transport Experiment (INTEX-B) to quantify long-range transport of East Asian sulfur to Canada, Atmos. Chem. Phys., 8(11), 2999–3014, doi:10.5194/acp-8-2999-2008, 2008.

Drury, E., Jacob, D. J., Spurr, R. J. D., Wang, J., Shinozuka, Y., Anderson, B. E., Clarke, A. D., Dibb, J., McNaughton, C. and Weber, R.: Synthesis of satellite (MODIS), aircraft (ICARTT), and surface (IMPROVE, EPA-AQS, AERONET) aerosol observations over eastern North

America to improve MODIS aerosol retrievals and constrain surface aerosol concentrations and sources, J. Geophys. Res., 115(D14), D14204, doi:10.1029/2009JD012629, 2010.

Duplissy, J., DeCarlo, P. F., Dommen, J., Alfarra, M. R., Metzger, A., Barmpadimos, I., Prevot, A. S. H., Weingartner, E., Tritscher, T., Gysel, M., Aiken, A. C., Jimenez, J. L., Canagaratna, M. R., Worsnop, D. R., Collins, D. R., Tomlinson, J. and Baltensperger, U.: Relating hygroscopicity and composition of organic aerosol particulate matter, Atmos. Chem. Phys., 11(3), 1155–1165, doi:10.5194/acp-11-1155-2011, 2011.

Fairlie, D. J., Jacob, D. J. and Park, R. J.: The impact of transpacific transport of mineral dust in the United States, Atmos. Environ., 41(6), 1251–1266, doi:10.1016/j.atmosenv.2006.09.048, 2007.

Feng, Y., Ramanathan, V. and Kotamarthi, V. R.: Brown carbon: A significant atmospheric absorber of solar radiation, Atmos. Chem. Phys., 13(17), 8607–8621, doi:10.5194/acp-13-8607-2013, 2013.

Flores, J. M., Washenfelder, R. A., Adler, G., Lee, H. J., Segev, L., Laskin, J., Laskin, A., Nizkorodov, S. A., Brown, S. S. and Rudich, Y.: Complex refractive indices in the near-ultraviolet spectral region of biogenic secondary organic aerosol aged with ammonia., Phys. Chem. Chem. Phys., 16(22), 10629–42, doi:10.1039/c4cp01009d, 2014.

Forrister, H., Liu, J., Scheuer, E., Dibb, J., Ziemba, L., Thornhill, K. L., Anderson, B., Diskin, G., Perring, A. E., Schwarz, J. P., Campuzano-Jost, P., Day, D. A., Palm, B. B., Jimenez, J. L., Nenes, A. and Weber, R. J.: Evolution of brown carbon in wildfire plumes, Geophys. Res. Lett., 42(11), 4623–4630, doi:10.1002/2015GL063897, 2015.

Fountoukis, C. and Nenes, A.: ISORROPIA II: a computationally efficient thermodynamic equilibrium model for K^+–Ca^{2+}–Mg^{2+}–NH_4^+–Na^+–SO_4^{2-}–NO_3^-–Cl^-–H_2O aero, Atmos. Chem. Phys., 7(17), 4639–4659, doi:10.5194/acp-7-4639-2007, 2007.

Hallquist, M., Wenger, J. C., Baltensperger, U., Rudich, Y., Simpson, D., Claeys, M., Dommen, J., Donahue, N. M., George, C., Goldstein, A. H., Hamilton, J. F., Herrmann, H., Hoffmann, T., Iinuma, Y., Jang, M., Jenkin, M. E., Jimenez, J. L., Kiendler-Scharr, A., Maenhaut, W., McFiggans, G., Mentel, T. F., Monod, A., Prévôt, A. S. H., Seinfeld, J. H., Surratt, J. D., Szmigielski, R. and Wildt, J.: The formation, properties and impact of secondary organic aerosol: current and emerging issues, Atmos. Chem. Phys., 9(14), 5155–5236, doi:10.5194/acp-9-5155-2009, 2009.

Heald, C. L., Ridley, D. A., Kroll, J. H., Barrett, S. R. H., Cady-Pereira, K. E., Alvarado, M. J. and Holmes, C. D.: Contrasting the direct radiative effect and direct radiative forcing of aerosols, Atmos. Chem. Phys., 14(11), 5513–5527, doi:10.5194/acp-14-5513-2014, 2014.

Henze, D. K. and Seinfeld, J. H.: Global secondary organic aerosol from isoprene oxidation, Geophys. Res. Lett., 33, L09812, 2006.

Henze, D. K., Seinfeld, J. H., Ng, N. L., Kroll, J. H., Fu, T.-M., Jacob, D. J. and Heald, C. L.: Global modeling of secondary organic aerosol formation from aromatic hydrocarbons: high- vs. low-yield pathways, Atmos. Chem. Phys., 8(9), 2405–2420, doi:10.5194/acp-8-2405-2008, 2008.

Herman, J. R., Bhartia, P. K., Torres, O., Hsu, C., Seftor, C. and Celarier, E.: Global distribution of UV-absorbing aerosols from Nimbus 7/TOMS data, J. Geophys. Res., 102(D14), 16911, doi:10.1029/96JD03680, 1997.

Iacono, M. J., Delamere, J. S., Mlawer, E. J., Shephard, M. W., Clough, S. A. and Collins, W. D.: Radiative forcing by long-lived greenhouse gases: Calculations with the AER radiative transfer models, J. Geophys. Res., 113(D13), D13103, doi:10.1029/2008JD009944, 2008.

IPCC: Climate Change 2014: Impacts, Adaptation, and Vulnerability. Part A: Global and Sectoral Aspects. Contribution of Working Group II to the Fifth Assessment Report of the Intergovernmental Panel on Climate Change [Field, C.B., V.R. Barros, D.J. Dokken, K.J., Cambridge University Press, Cambridge, United Kingdom and New York, NY, USA., 2014.

Jacobson, M. Z.: Studying the effects of aerosols on vertical photolysis rate coefficient and temperature profiles over an urban airshed, J. Geophys. Res., 103(D9), 10593, doi:10.1029/98JD00287, 1998.

Jaeglé, L., Quinn, P. K., Bates, T. S., Alexander, B. and Lin, J.-T.: Global distribution of sea salt aerosols: new constraints from in situ and remote sensing observations, Atmos. Chem. Phys., 11(7), 3137–3157, doi:10.5194/acp-11-3137-2011, 2011.

Jethva, H. and Torres, O.: Satellite-based evidence of wavelength-dependent aerosol absorption in biomass burning smoke inferred from Ozone Monitoring Instrument, Atmos. Chem. Phys., 11(20), 10541–10551, doi:10.5194/acp-11-10541-2011, 2011.

Jo, D. S., Park, R. J., Lee, S., Kim, S.-W. and Zhang, X.: A global simulation of brown carbon: implications for photochemistry and direct radiative effect, Atmos. Chem. Phys. Discuss., 15(19), 27805–27852, doi:10.5194/acpd-15-27805-2015, 2015.

Kirchstetter, T. W. and Thatcher, T. L.: Contribution of organic carbon to wood smoke particulate matter absorption of solar radiation, Atmos. Chem. Phys., 12(14), 6067–6072, doi:10.5194/acp-12-6067-2012, 2012.

Kirchstetter, T. W., Novakov, T. and Hobbs, P. V.: Evidence that the spectral dependence of light absorption by aerosols is affected by organic carbon, J. Geophys. Res. D Atmos., 109(21), D21208, doi:10.1029/2004JD004999, 2004.

Koepke, P., Hess, M., Schult, I. and Shettle, E. P.: Global Aerosol Dataset, report, Max-Planck Inst. fur Meteorol., Hamburg, Germany., 1997.

Kuhns, H., Knipping, E. M. and Vukovich, J. M.: Development of a United States–Mexico Emissions Inventory for the Big Bend Regional Aerosol and Visibility Observational (BRAVO) Study, J. Air Waste Manage. Assoc., 55(5), 677–692, doi:10.1080/10473289.2005.10464648, 2005.

Kuwata, M., Zorn, S. R. and Martin, S. T.: Using elemental ratios to predict the density of organic material composed of carbon, hydrogen, and oxygen., Environ. Sci. Technol., 46(2), 787–94, doi:10.1021/es202525q, 2012.

Lack, D. A. and Langridge, J. M.: On the attribution of black and brown carbon light absorption using the Ångström exponent, Atmos. Chem. Phys., 13(20), 10535–10543, doi:10.5194/acp-13-10535-2013, 2013.

Lack, D. A., Tie, X. X., Bofinger, N. D., Wiegand, A. N. and Madronich, S.: Seasonal variability of secondary organic aerosol: A global modeling study, J. Geophys. Res., 109(D3), D03203, doi:10.1029/2003JD003418, 2004.

Lee, C., Martin, R. V., van Donkelaar, A., O'Byrne, G., Krotkov, N., Richter, A., Huey, L. G. and Holloway, J. S.: Retrieval of vertical columns of sulfur dioxide from SCIAMACHY and

OMI: Air mass factor algorithm development, validation, and error analysis, J. Geophys. Res., 114(D22), D22303, doi:10.1029/2009JD012123, 2009.

Leibensperger, E. M., Mickley, L. J., Jacob, D. J., Chen, W.-T., Seinfeld, J. H., Nenes, A., Adams, P. J., Streets, D. G., Kumar, N. and Rind, D.: Climatic effects of 1950–2050 changes in US anthropogenic aerosols – Part 2: Climate response, Atmos. Chem. Phys., 12(7), 3349–3362, doi:10.5194/acp-12-3349-2012, 2012.

Liao, H., Adams, P. J., Chung, S. H., Seinfeld, J. H., Mickley, L. J. and Jacob, D. J.: Interactions between tropospheric chemistry and aerosols in a unified general circulation model, J. Geophys. Res., 108(D1), 4001, doi:10.1029/2001JD001260, 2003.

Liao, H., Henze, D. K., Seinfeld, J. H., Wu, S. and Mickley, L. J.: Biogenic secondary organic aerosol over the United States: Comparison of climatological simulations with observations, J. Geophys. Res., 112(D6), D06201, doi:10.1029/2006JD007813, 2007.

Lin, G., Penner, J. E., Flanner, M. G., Sillman, S., Xu, L. and Zhou, C.: Radiative forcing of organic aerosol in the atmosphere and on snow: Effects of SOA and brown carbon, J. Geophys. Res. Atmos., 119(12), 7453–7476, doi:10.1002/2013JD021186, 2014.

Liu, J., Bergin, M., Guo, H., King, L., Kotra, N., Edgerton, E. and Weber, R. J.: Size-resolved measurements of brown carbon in water and methanol extracts and estimates of their contribution to ambient fine-particle light absorption, Atmos. Chem. Phys., 13(24), 12389–12404, doi:10.5194/acp-13-12389-2013, 2013.

Liu, J., Scheuer, E., Dibb, J., Diskin, G. S., Ziemba, L. D., Thornhill, K. L., Anderson, B. E., Wisthaler, A., Mikoviny, T., Devi, J. J., Bergin, M., Perring, A. E., Markovic, M. Z., Schwarz, J. P., Campuzano-Jost, P., Day, D. A., Jimenez, J. L. and Weber, R. J.: Brown carbon aerosol in the North American continental troposphere: sources, abundance, and radiative forcing, Atmos. Chem. Phys., 15(14), 7841–7858, doi:10.5194/acp-15-7841-2015, 2015.

Liu, P. F., Abdelmalki, N., Hung, H.-M., Wang, Y., Brune, W. H. and Martin, S. T.: Ultraviolet and visible complex refractive indices of secondary organic material produced by photooxidation of the aromatic compounds toluene and *m*-Xylene, Atmos. Chem. Phys. Discuss., 14(14), 20585–20615, doi:10.5194/acpd-14-20585-2014, 2014.

Mao, J., Fan, S., Jacob, D. J. and Travis, K. R.: Radical loss in the atmosphere from Cu-Fe redox coupling in aerosols, Atmos. Chem. Phys., 13(2), 509–519, doi:10.5194/acp-13-509-2013, 2013.

Martin, R. V., Jacob, D. J., Yantosca, R. M., Chin, M. and Ginoux, P.: Global and regional decreases in tropospheric oxidants from photochemical effects of aerosols, J. Geophys. Res., 108(D3), 4097, doi:10.1029/2002JD002622, 2003.

Martins, J. V., Artaxo, P., Kaufman, Y. J., Castanho, A. D. and Remer, L. A.: Spectral absorption properties of aerosol particles from 350–2500nm, Geophys. Res. Lett., 36(13), 1–5, doi:10.1029/2009GL037435, 2009.

Mu, M., Randerson, J. T., van der Werf, G. R., Giglio, L., Kasibhatla, P., Morton, D., Collatz, G. J., DeFries, R. S., Hyer, E. J., Prins, E. M., Griffith, D. W. T., Wunch, D., Toon, G. C., Sherlock, V. and Wennberg, P. O.: Daily and 3-hourly variability in global fire emissions and consequences for atmospheric model predictions of carbon monoxide, J. Geophys. Res. Atmos., 116(D24), D24303, doi:10.1029/2011JD016245, 2011.

Naik, V., Voulgarakis, A., Fiore, A. M., Horowitz, L. W., Lamarque, J.-F., Lin, M., Prather, M.

J., Young, P. J., Bergmann, D., Cameron-Smith, P. J., Cionni, I., Collins, W. J., Dalsøren, S. B., Doherty, R., Eyring, V., Faluvegi, G., Folberth, G. A., Josse, B., Lee, Y. H., MacKenzie, I. A., Nagashima, T., van Noije, T. P. C., Plummer, D. A., Righi, M., Rumbold, S. T., Skeie, R., Shindell, D. T., Stevenson, D. S., Strode, S., Sudo, K., Szopa, S. and Zeng, G.: Preindustrial to present-day changes in tropospheric hydroxyl radical and methane lifetime from the Atmospheric Chemistry and Climate Model Intercomparison Project (ACCMIP), Atmos. Chem. Phys., 13(10), 5277–5298, doi:10.5194/acp-13-5277-2013, 2013.

Olivier, J. G. J., Van Aardenne, J. A., Dentener, F. J., Pagliari, V., Ganzeveld, L. N. and Peters, J. A. H. W.: Recent trends in global greenhouse gas emissions:regional trends 1970–2000 and spatial distributionof key sources in 2000, Environ. Sci., 2(2-3), 81–99, doi:10.1080/15693430500400345, 2005.

Park, R. J., Jacob, D. J., Chin, M. and Martin, R. V.: Sources of carbonaceous aerosols over the United States and implications for natural visibility, J. Geophys. Res., 108(D12), 4355, doi:10.1029/2002JD003190, 2003.

Park, R. J., Jacob, D. J., Field, B. D., Yantosca, R. M. and Chin, M.: Natural and transboundary pollution influences on sulfate-nitrate-ammonium aerosols in the United States: Implications for policy, J. Geophys. Res., 109(D15), D15204, doi:10.1029/2003JD004473, 2004.

Park, R. J., Kim, M. J., Jeong, J. I., Youn, D. and Kim, S.: A contribution of brown carbon aerosol to the aerosol light absorption and its radiative forcing in East Asia, Atmos. Environ., 44(11), 1414–1421, doi:10.1016/j.atmosenv.2010.01.042, 2010.

Prather, M. J., Holmes, C. D. and Hsu, J.: Reactive greenhouse gas scenarios: Systematic exploration of uncertainties and the role of atmospheric chemistry, Geophys. Res. Lett., 39(9), L09803, doi:10.1029/2012GL051440, 2012.

Prinn, R. G., Huang, J., Weiss, R. F., Cunnold, D. M., Fraser, P. J., Simmonds, P. G., McCulloch, A., Harth, C., Reimann, S., Salameh, P., O'Doherty, S., Wang, R. H. J., Porter, L. W., Miller, B. R. and Krummel, P. B.: Evidence for variability of atmospheric hydroxyl radicals over the past quarter century, Geophys. Res. Lett., 32(7), L07809, doi:10.1029/2004GL022228, 2005.

Pye, H. O. T., Liao, H., Wu, S., Mickley, L. J., Jacob, D. J., Henze, D. K. and Seinfeld, J. H.: Effect of changes in climate and emissions on future sulfate-nitrate-ammonium aerosol levels in the United States, J. Geophys. Res., 114(D1), D01205, doi:10.1029/2008JD010701, 2009.

Ramanathan, V. and Carmichael, G.: Global and regional climate changes due to black carbon, Nat. Geosci., 1(4), 221–227, doi:10.1038/ngeo156, 2008.

Ridley, D. A., Heald, C. L. and Ford, B.: North African dust export and deposition: A satellite and model perspective, J. Geophys. Res., 117(D2), D02202, doi:10.1029/2011JD016794, 2012.

Rizzo, L. V., Correia, A. L., Artaxo, P., Procápio, A. S. and Andreae, M. O.: Spectral dependence of aerosol light absorption over the Amazon Basin, Atmos. Chem. Phys., 11(17), 8899–8912, doi:10.5194/acp-11-8899-2011, 2011.

Russell, P. B., Bergstrom, R. W., Shinozuka, Y., Clarke, A. D., DeCarlo, P. F., Jimenez, J. L., Livingston, J. M., Redemann, J., Holben, B., Dubovik, O. and Strawa, A.: Absorption Angstrom Exponent in AERONET and related data as an indicator of aerosol composition, Atmos. Chem. Phys. Discuss., 9(5), 21785–21817, doi:10.5194/acpd-9-21785-2009, 2009.

Saleh, R., Robinson, E. S., Tkacik, D. S., Ahern, A. T., Liu, S., Aiken, A. C., Sullivan, R. C., Presto, A. A., Dubey, M. K., Yokelson, R. J., Donahue, N. M. and Robinson, A. L.: Brownness of organics in aerosols from biomass burning linked to their black carbon content, Nat. Geosci., 7(9), 647–650, doi:10.1038/ngeo2220, 2014.

Spivakovsky, C. M., Logan, J. A., Montzka, S. A., Balkanski, Y. J., Foreman-Fowler, M., Jones, D. B. A., Horowitz, L. W., Fusco, A. C., Brenninkmeijer, C. A. M., Prather, M. J., Wofsy, S. C. and McElroy, M. B.: Three-dimensional climatological distribution of tropospheric OH: Update and evaluation, J. Geophys. Res., 105(D7), 8931, doi:10.1029/1999JD901006, 2000.

Spurr, R. J. D.: VLIDORT: A linearized pseudo-spherical vector discrete ordinate radiative transfer code for forward model and retrieval studies in multilayer multiple scattering media, J. Quant. Spectrosc. Radiat. Transf., 102(2), 316–342, doi:10.1016/j.jqsrt.2006.05.005, 2006.

Stier, P., Seinfeld, J. H., Kinne, S. and Boucher, O.: Aerosol absorption and radiative forcing, Atmos. Chem. Phys., 7(19), 5237–5261, doi:10.5194/acp-7-5237-2007, 2007.

Sun, H., Biedermann, L. and Bond, T. C.: Color of brown carbon: A model for ultraviolet and visible light absorption by organic carbon aerosol, Geophys. Res. Lett., 34(17), L17813, doi:10.1029/2007GL029797, 2007.

Torres, O., Bhartia, P. K., Herman, J. R., Ahmad, Z. and Gleason, J.: Derivation of aerosol properties from satellite measurements of backscattered ultraviolet radiation: Theoretical basis, J. Geophys. Res., 103(D14), 17099, doi:10.1029/98JD00900, 1998.

Torres, O., Bhartia, P. K., Sinyuk, A., Welton, E. J. and Holben, B.: Total Ozone Mapping Spectrometer measurements of aerosol absorption from space: Comparison to SAFARI 2000 ground-based observations, J. Geophys. Res., 110(D10), D10S18, doi:10.1029/2004JD004611, 2005.

Torres, O., Tanskanen, A., Veihelmann, B., Ahn, C., Braak, R., Bhartia, P. K., Veefkind, P. and Levelt, P.: Aerosols and surface UV products from Ozone Monitoring Instrument observations: An overview, J. Geophys. Res., 112(D24), D24S47, doi:10.1029/2007JD008809, 2007.

Torres, O., Ahn, C. and Chen, Z.: Improvements to the OMI near-UV aerosol algorithm using A-train CALIOP and AIRS observations, Atmos. Meas. Tech., 6(11), 3257–3270, doi:10.5194/amt-6-3257-2013, 2013.

Tsigaridis, K. and Kanakidou, M.: Global modelling of secondary organic aerosol in the troposphere: a sensitivity analysis, Atmos. Chem. Phys., 3(5), 1849–1869, doi:10.5194/acp-3-1849-2003, 2003.

Turpin, B. J. and Lim, H.-J.: Species Contributions to PM2.5 Mass Concentrations: Revisiting Common Assumptions for Estimating Organic Mass, Aerosol Sci. Technol., 35(1), 602–610, doi:10.1080/02786820119445, 2001.

Wang, X., Heald, C. L., Ridley, D. A., Schwarz, J. P., Spackman, J. R., Perring, A. E., Coe, H., Liu, D. and Clarke, A. D.: Exploiting simultaneous observational constraints on mass and absorption to estimate the global direct radiative forcing of black carbon and brown carbon, Atmos. Chem. Phys., 14(20), 10989–11010, doi:10.5194/acp-14-10989-2014, 2014.

Yang, M., Howell, S. G., Zhuang, J. and Huebert, B. J.: Attribution of aerosol light absorption to black carbon, brown carbon, and dust in China- interpretations of atmospheric measurements during EAST-AIRE, Atmos. Chem. Phys. Discuss., 8(3), 10913–10954, doi:10.5194/acpd-8-

10913-2008, 2008.

Yevich, R. and Logan, J. A.: An assessment of biofuel use and burning of agricultural waste in the developing world, Global Biogeochem. Cycles, 17(4), 1095, doi:10.1029/2002GB001952, 2003.

Zhang, L., Jacob, D. J., Kopacz, M., Henze, D. K., Singh, K. and Jaffe, D. A.: Intercontinental source attribution of ozone pollution at western U.S. sites using an adjoint method, Geophys. Res. Lett., 36, L11810 [online] Available from: http://dash.harvard.edu/handle/1/3627131 (Accessed 9 May 2015), 2009.

Zhang, X., Lin, Y.-H., Surratt, J. D. and Weber, R. J.: Sources, composition and absorption Ångström exponent of light-absorbing organic components in aerosol extracts from the Los Angeles Basin., Environ. Sci. Technol., 47(8), 3685–93, doi:10.1021/es305047b, 2013.

Zhong, M. and Jang, M.: Dynamic light absorption of biomass-burning organic carbon photochemically aged under natural sunlight, Atmos. Chem. Phys., 14(3), 1517–1525, doi:10.5194/acp-14-1517-2014, 2014.

Tables and Figures

Table 1: Absorption Angstrom Exponent (AAE) values for biomass burning regions from the literature.

Wavelength (nm)	AAE value	Region	Reference
350-400 nm			
350-400	2.5-3.0	South America	Jethva and Torres, 2011
350-700 nm			
360-700	1.9	Rural California	Kirchstetter and Thatcher, 2012
450-550 nm			
470-532	1.9	North-central Canada	Corr et al. 2012
470-532	1.4	"	"
Mean ± SD* = 1.7 ± 0.35			
400-700 nm			
400-700	1.5-1.9	Laboratory	Schnaiter et al. 2005
440-670	1.8	Boreal Forest	Russell et al. 2010
440-670	1.3	Southern Africa	"
440-670	1.4	South America	"
440-670	1.6	Amazon	"
470-660	1.7	Arctic	Corr et al. 2012
470-660	1.3	Arctic	"
470-660	1.5	Outside Beijing	Yang et al. 2009
470-660	2.1	North America	Clarke et al. 2007
Mean ± SD = 1.6 ±0.26			
450-700 nm			
470-660	2.2	North America	Liu et al. 2015
300-1000 nm			
325-1000	1.1	Southern Africa	Bergstrom et al. 2007
325-1685	1.5	Southern Africa	"
330-1000	2	Southern Africa	Kirchstetter et al. 2004
370-950	1.5	Outside Beijing	Yang et al. 2009
Mean ± SD = 1.5 ± 0.37			
400-1000 nm			
440-870	1.6	Boreal Forest	Russell et al. 2010
440-870	1.3	Southern Africa	"
440-870	1.4	South America	"
440-870	1.4	Amazon	"
440-1020	1.5	Boreal Forest	"
440-1020	1.3	Southern Africa	"
440-1020	1.3	South America	"
440-1020	1.4	Amazon	"
450-950	1.7	Amazon	Rizzo et al. 2011
Mean ± SD = 1.4 ± 0.14			

***SD: standard deviation**

Table 2: Imaginary part of the refractive index (*k*) values for the base case with weakly absorbing "colorless" primary organic carbon.

Wavelength (nm)	**Base Case**
300	0.008
350	0.005
400	0.005
450	0.005
500	0.005
550	0.006

Table 3: Comparison of the simulated versus observed (OMI) UVAI values for the biomass burning regions in the months examined. The base case corresponds to a simulation without BrC, while Case 2 corresponds to a simulation including absorbing BrC.

Region[d]	n[c]	Month	Mean OMI UVAI	Base Case r[a]	Base Case Mean Bias[b]	Case 2 with BrC r	Case 2 with BrC Mean Bias
West Africa	381	January	1.25	0.48	-0.57	0.68	-0.09
South Asia	280	April	0.34	0.46	-0.32	0.66	+0.0002
Southern Africa	184	July	0.66	0.09	-0.97	0.63	-0.22
South America	230	September	0.30	0.40	-0.50	0.57	+0.33

[a] r: Pearson correlation coefficient

[b] Mean bias = simulated UVAI – observed UVAI

[c] n = number of GEOS-Chem grid boxes in region

[d] regions are defined in Figure 1

Table 4: The mean AOD values for each region from the GEOS-Chem (GC) base case simulation, the MISR instrument, and the MODIS Terra satellite instrument. The MODIS values are included for both the collection 6 Deep Blue and Dark Target algorithms.

			Mean AOD	
Region[a]	**GC**	**MISR**	**MODIS Deep Blue**	**MODIS Dark Target**
West Africa	0.42	0.42	0.45	0.51
South Asia	0.32	0.32	0.30	0.37
Southern Africa	0.19	0.19	0.13	0.24
South America	0.31	0.36	0.39	0.57

[a] regions are defined in Figure 1

Table 5: Imaginary part of the refractive index (*k*) values for brown carbon (not total organic carbon) inferred for case 2.~~the base case with weakly absorbing "white" organic carbon, and case 2 with brown carbon. Case 2 includes~~ We include *k* values associated with multiple densities (ρ), and multiple fractions of brown carbon to primary organic carbon (BrC/POC). All four columns for case 2 yield the same absorption.

	Case 2 with BrC (ρ = 1.3 g cm^{-3})		**Case 2 with BrC (ρ = 1.8 g cm^{-3})**	
Wavelength (nm)	**BrC/POC = 0.50**	**BrC/POC = 1.0**	**BrC/POC = 0.50**	**BrC/POC=1.0**
300	0.11	0.051	0.16	0.071
350	0.077	0.037	0.11	0.051
400	0.052	0.025	0.073	0.035
450	0.035	0.014	0.049	0.019
500	0.023	0.009	0.032	0.013
550	0.015	0.007	0.021	0.010

Table 6: The Absorption Angstrom Exponent (AAE) values for major biomass burning regions and seasons obtained from the base case simulation ~~assuming non-absorbing organic carbon~~without BrC and the case 2 simulation including absorbing BrC.

Wavelength (nm)	January (West Africa)	April (South Asia)	July (Southern Africa)	September (South America)	Mean ± SD*
Base Case					
350-400	1.2	1.2	1.2	1.2	1.2 ± 0.00
350-700	1.0	1.2	1.0	1.1	1.1 ± 0.09
450-550	0.8	1.1	0.7	1.0	0.9 ± 0.18
400-700	1.0	1.2	0.9	1.1	1.1 ± 0.13
450-700	1.0	1.1	0.9	1.0	1.0 ± 0.08
300-1000	0.9	1.1	0.9	0.9	0.9 ± 0.10
400-1000	0.7	0.9	0.7	0.7	0.8 ± 0.10
Case 2 with BrC					
350-400	2.9	2.5	3	2.9	2.8 ± 0.22
350-700	2.3	2	2.4	2.3	2.2 ± 0.17
450-550	2.5	2.3	2.6	2.6	2.5 ± 0.14
400-700	2.2	1.9	2.2	2.2	2.1 ± 0.15
450-700	1.9	1.7	1.9	1.9	1.8 ± 0.10
300-1000	1.8	1.6	1.8	1.8	1.7 ± 0.15
400-1000	1.3	1.3	1.3	1.3	1.3 ± 0.00

*SD: standard deviation

Table 7: Global annual mean LW and SW flux differences and resulting DRE values for 2007 at TOA and the surface. The values for organic aerosol are shown for both the base case simulation without BrC ~~non-absorbing organic carbon~~ and the case 2 simulation including absorbing brown carbon. The DRE values for BrC absorption are calculated as the difference between the DRE of organic aerosol from case 2 minus the base case.

	Organic Aerosol		**BrC Absorption**
	Base Case	**Case 2**	**Case 2 – Base Case**
TOA DRE, Clear Sky (Wm^{-2})	-0.23	-0.22	+0.01
LW	+0.0019	+0.0019	
SW	-0.23	-0.22	
TOA DRE, All Sky (Wm^{-2})	-0.17	-0.15	+0.02
LW	+0.0013	+0.0015	
SW	-0.17	-0.15	
Surface DRE, Clear Sky (Wm^{-2})	-0.36	-0.42	-0.07
LW	+0.0043	+0.0048	
SW	-0.36	-0.43	
Surface DRE, All Sky (Wm^{-2})	-0.29	-0.35	-0.06
LW	0.0036	0.0040	
SW	-0.29	-0.35	

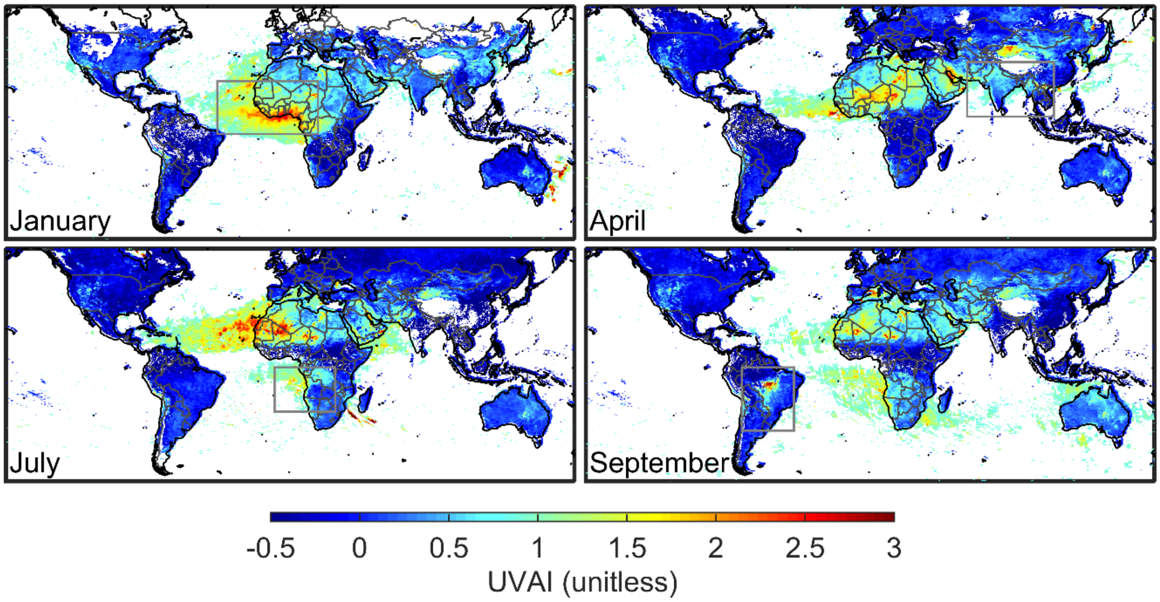

Figure 1: Monthly mean Ultraviolet Aerosol Index (UVAI) observations from the OMI satellite instrument for 2007. White space indicates cloud or snow contamination. Grey boxes outline regions examined in Tables 3 and 4.

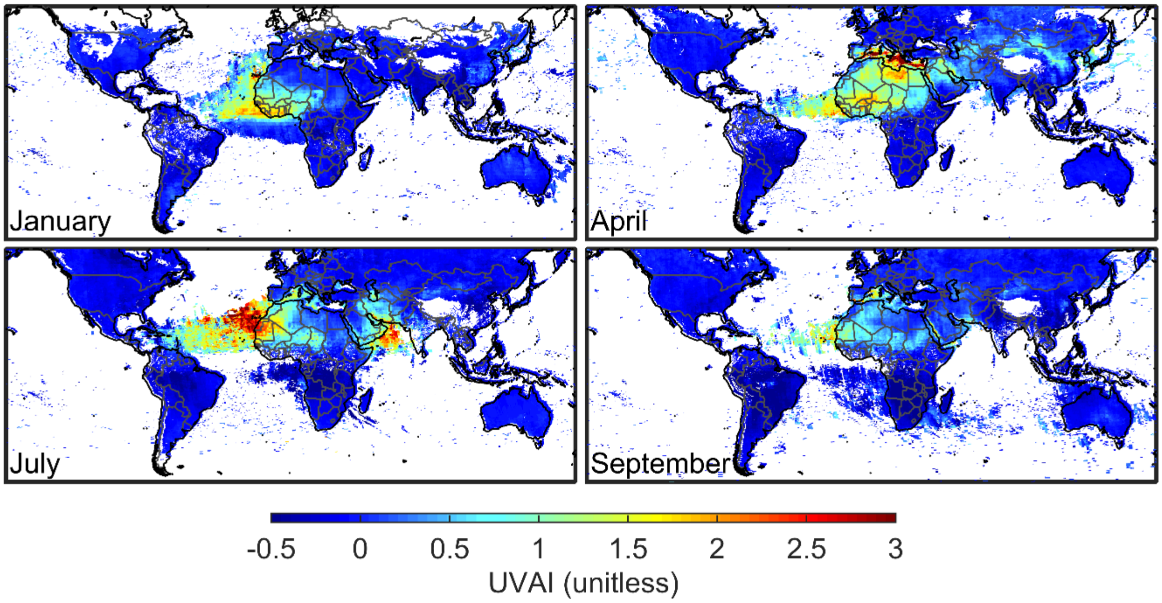

Figure 2: Monthly mean UVAI values for 2007 simulated for OMI observing conditions using the vector radiative transfer model VLIDORT coupled with GEOS-Chem aerosol fields for the base case without brown carbon (BrC)~~, which treats organic carbon aerosol as non-absorbing, for 2007~~. White ~~space~~ indicates cloud or snow contamination.

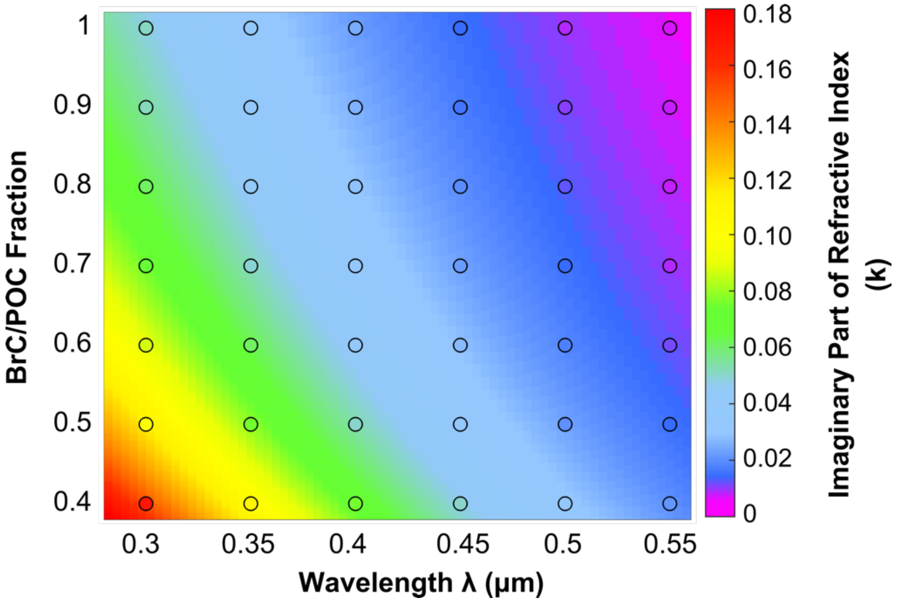

Figure 3: Imaginary part of the refractive index (*k*) values inferred for BrC as a function of wavelength and of the assumed fraction of primary organic carbon that is brown (BrC/POC). The background spectrum represents *k* values calculated using Eq. (6). The filled circles represent the *k* values obtained from sensitivity simulations. An organic carbon density of 1.3 g cm^{-3} is assumed.

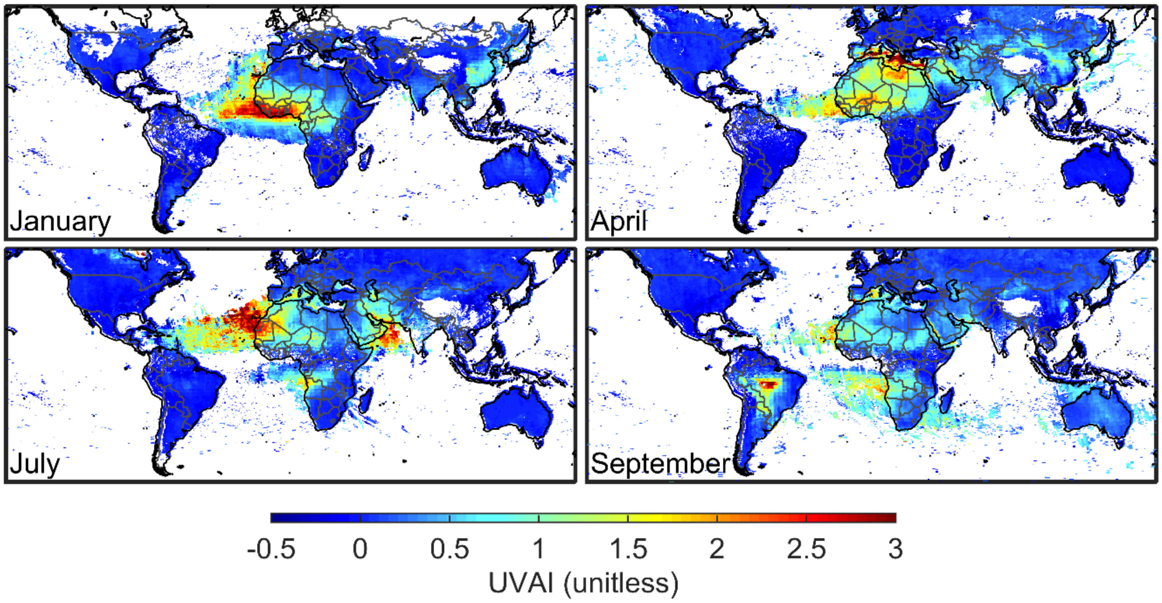

Figure 4: Monthly mean UVAI values for 2007 simulated for OMI observing conditions using the vector radiative transfer model VLIDORT coupled with GEOS-Chem aerosol fields for case 2, which assumes the presence of absorbing BrC aerosol. White ~~space~~ indicates clouds or snow contamination.

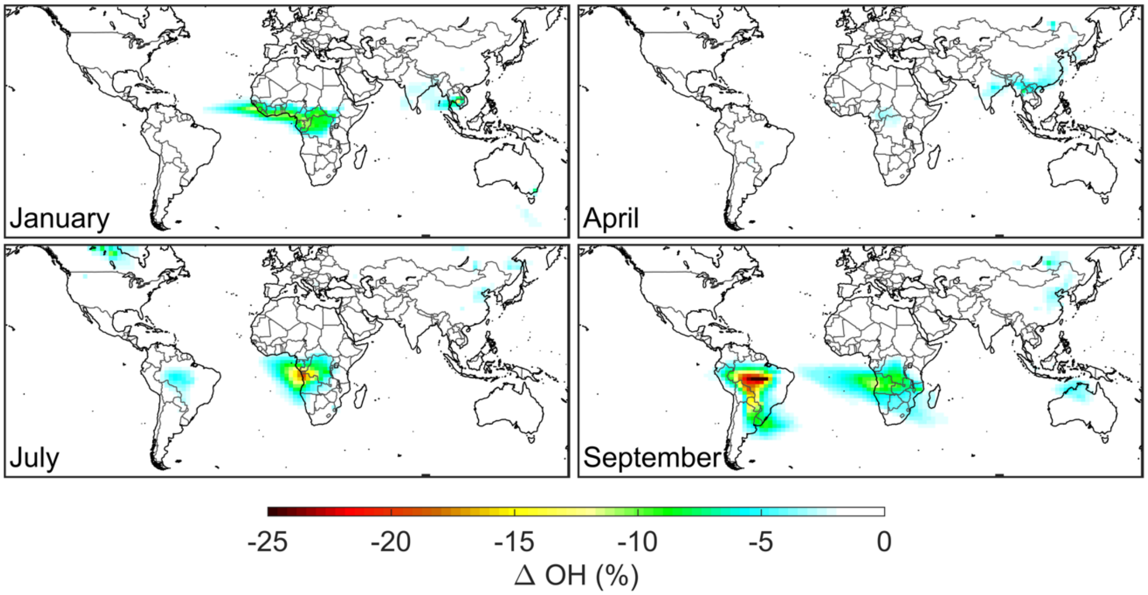

Figure 5: Percent difference between OH concentrations in the lower troposphere from a GEOS-Chem simulation including absorbing BrC minus a simulation~~ including non-absorbing organic carbon~~without BrC. The values are monthly means for January, April, July, and September of 2007.

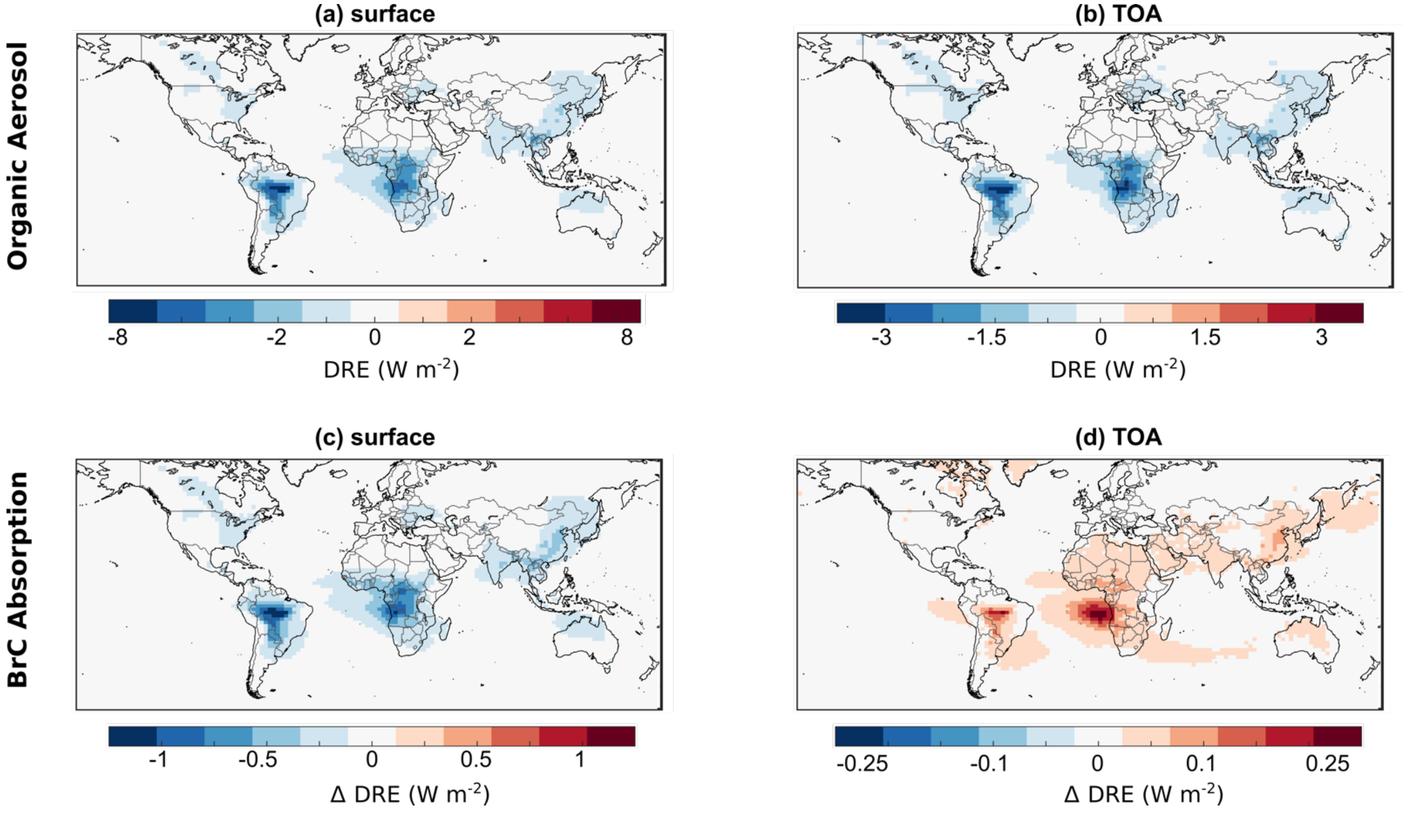

Figure 6: Annual mean all-sky DRE values for 2007 (Wm^{-2}). The top two panels are the DRE values for organic aerosol from the case 2 simulation including BrC at a) the surface and b) TOA. The bottom two panels are the change in DRE values for absorption by BrC calculated as the difference between the DRE values for organic aerosol from the case 2 simulation and the base case simulation (without BrC~~assuming non-absorbing organic carbon~~) at c) the surface and d) TOA.